$\gamma\gamma$ Colliders

ALEGRO 2025 Workshop

Tim Barklow

March 05, 2025

Outline

- Introduction to $\gamma\gamma$ Colliders
- $\gamma\gamma$ Collider Higgs Factories
- Multi-TeV $\gamma\gamma$ Colliders
- Future Work

XCC layout of 1 keV XFEL , 63 GeV e^- Beams near Interaction Point

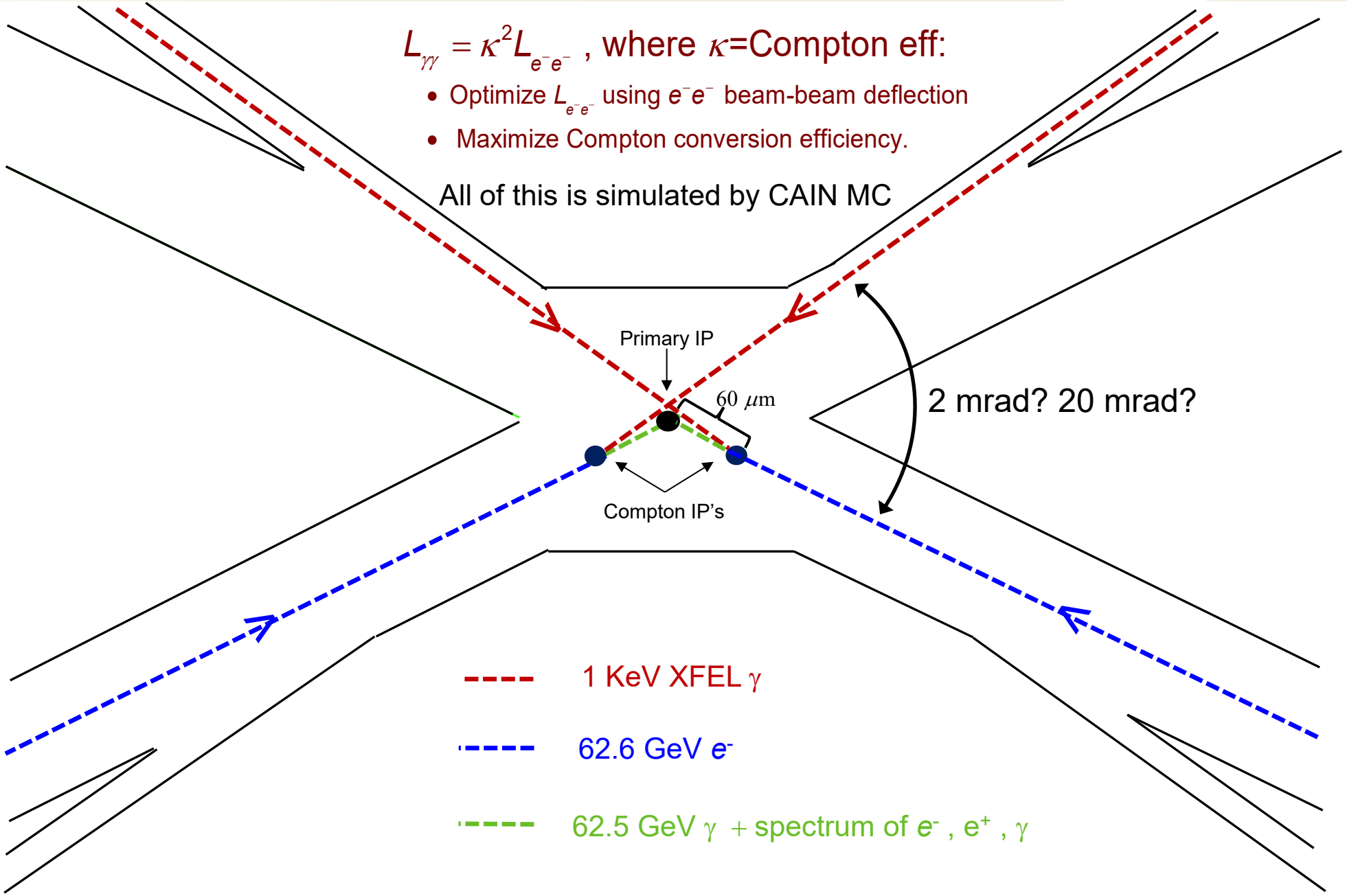

Optical → X-ray Laser Produces Narrower $\gamma\gamma$ Luminosity Spectra

$x = \frac{4E_{e^-}\omega_0}{m_e^2}$ determines luminosity spectra

$\omega_0 =$ laser photon energy

maximum Compton photon energy $\omega_m = \frac{x}{x+1}E_{e^-}$

angle scattered photon & electron $\theta_0 = \frac{m_e}{E_{e^-}}\sqrt{x+1}$

Important thresholds in x :

At $x = 4.82$ $\gamma\gamma_{\text{laser}} \to e^+e^-$ opens up which depletes the high energy photon beam.

At $x = 8$ $e^-\gamma_{\text{laser}} \to e^-e^+e^-$ opens up which increases e^- energy spread.

κ= 1 – prob that Compton γ annihilates with laser γ

$$\sigma(\gamma\gamma \to H) = \frac{8\pi\Gamma_{\gamma\gamma}\Gamma_{tot}}{(s-M_H^2)^2+\Gamma_{tot}^2M_H^2}(1+\xi_1\xi_2) \approx \frac{4\pi^2\Gamma_{\gamma\gamma}}{M_H^3}(1+\xi_1\xi_2)z_H\delta(z-z_H)$$

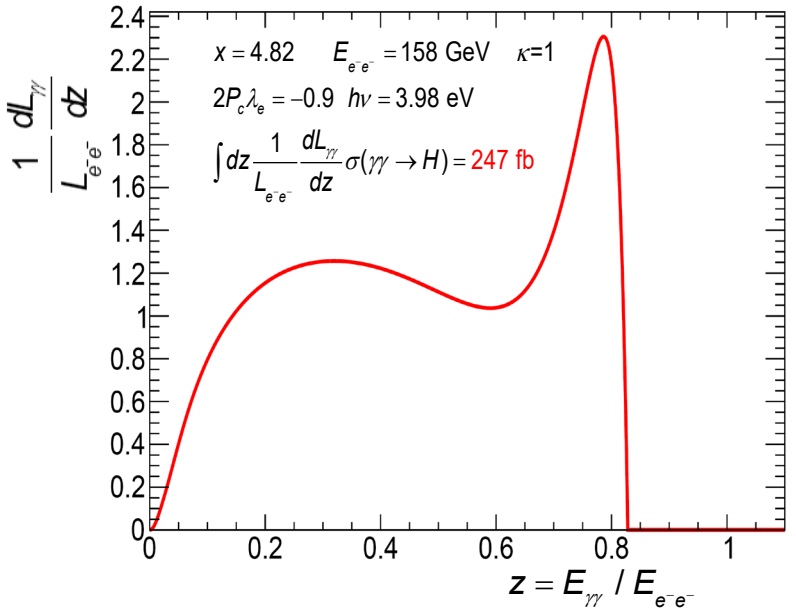

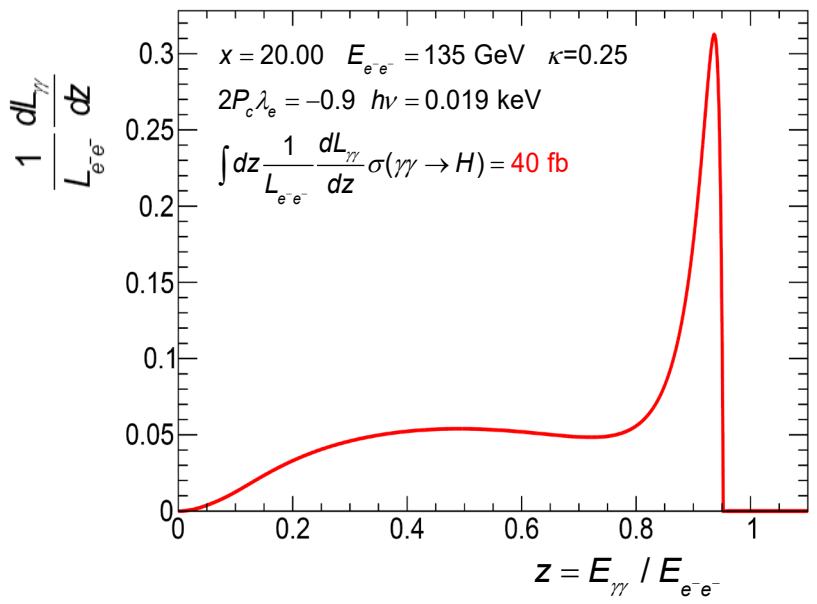

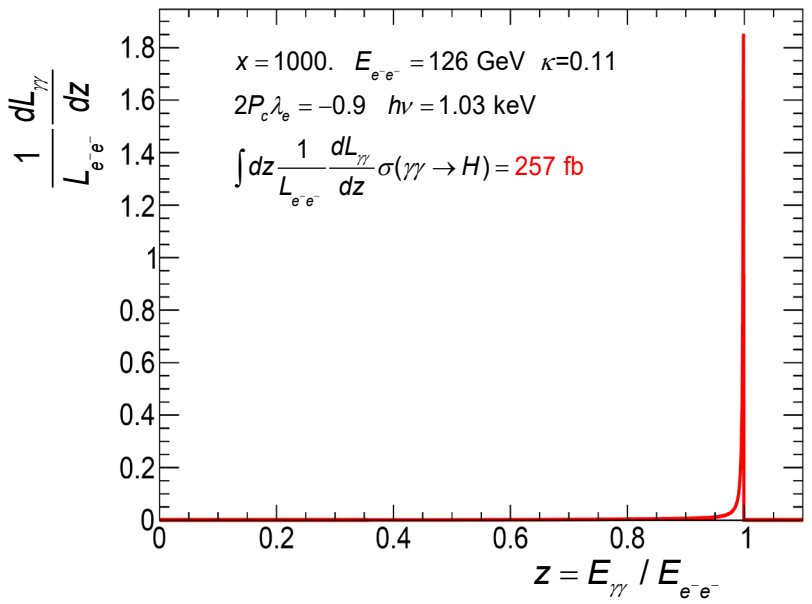

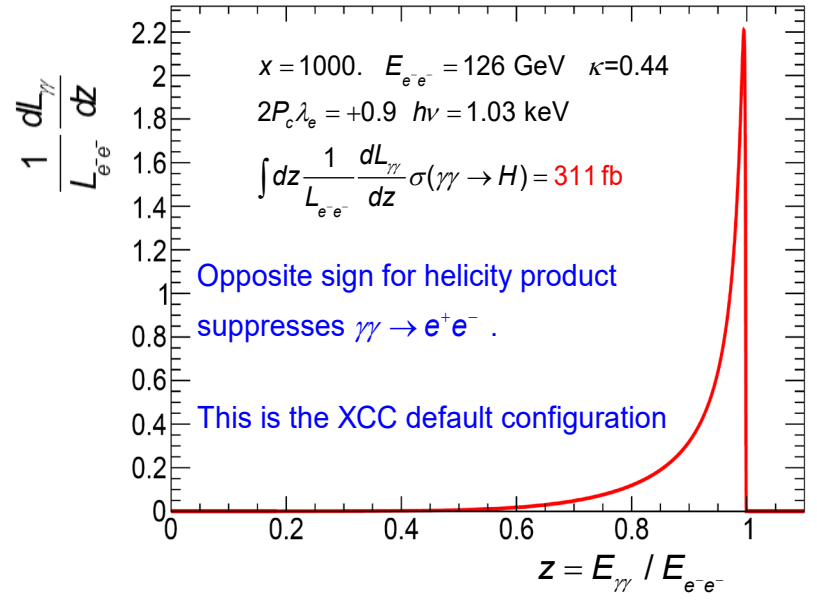

X-ray vs. Optical Laser $\gamma\gamma$ Higgs Factories $\sqrt{s} \approx 125$ GeV $(\gamma\gamma \to H)$

Linac	Laser E_γ (eV)	$\sqrt{s_{ee}}$ (GeV)	N_{bunch} / train	Rep Rate (Hz)	$L_{\gamma\gamma}$ $(cm^{-2}s^{-1})^\dagger$	$N_H/1.0\times10^7$s
SCRF	1.17	216	2820	5	3.5×10^{34}	25,000
C3	1.04×10^3	126	165	120	3.5×10^{34}	72,200

$^\dagger 0 < \sqrt{s_{\gamma\gamma}} < \sqrt{s_{ee}}$

C3 + XFEL a.k.a XFEL Compton Collider or XCC

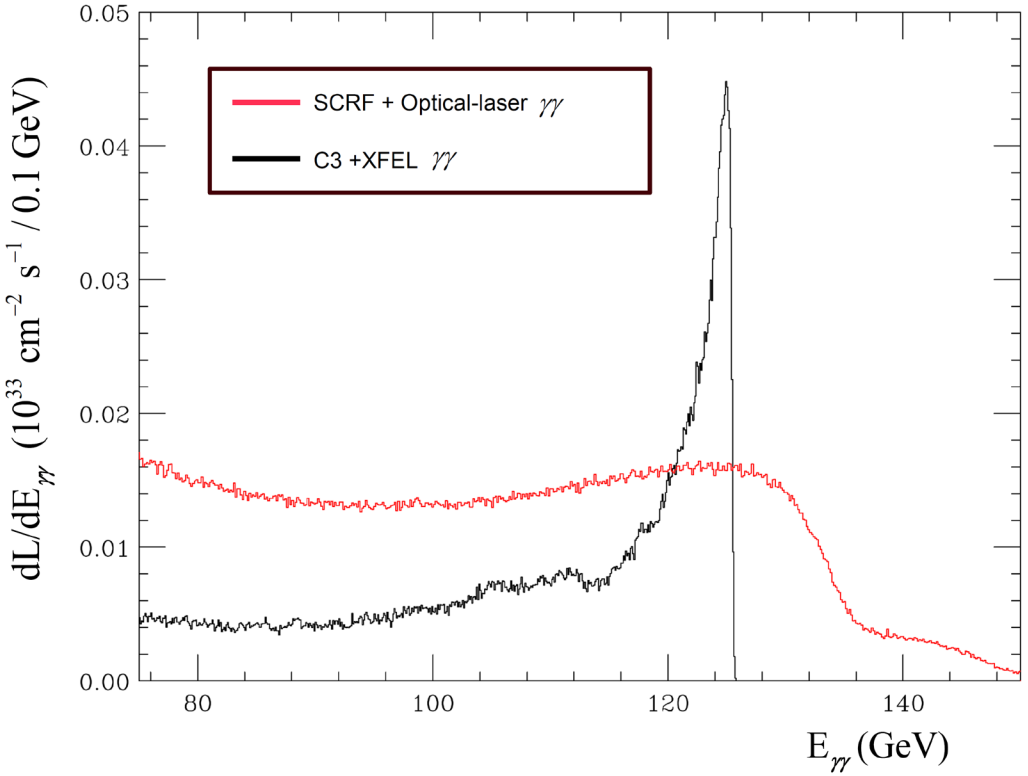

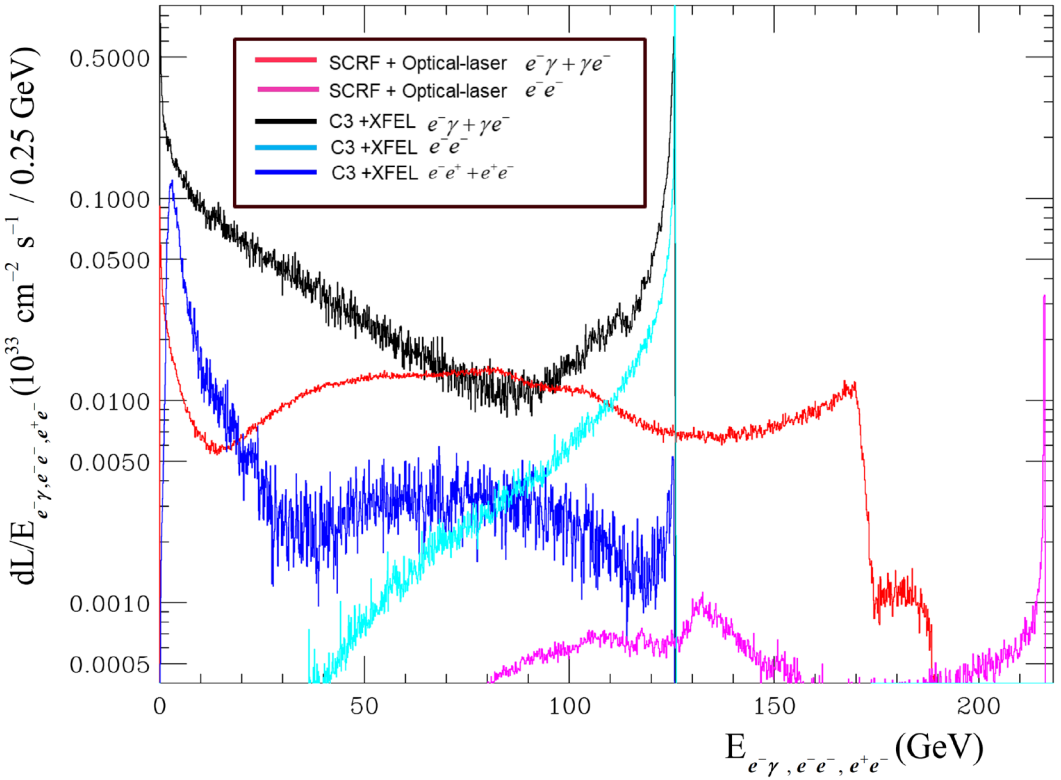

Comparison a bit unfair since XFEL collider requires much broader R&D program

X-ray vs. Optical Laser $\gamma\gamma$ Higgs Factories $\sqrt{s} \approx 380$ GeV $(\gamma\gamma \to HH)$

Linac	Laser E_γ (eV)	$\sqrt{s_{ee}}$ (GeV)	N_{bunch} / train	Rep Rate (Hz)	$L_{\gamma\gamma}$ ($cm^{-2}s^{-1}$)†	$N_{HH}/1.0\times10^7$s
SCRF	1.17	500	2820	5	0.73×10^{35}	20
C3	0.52×10^3	380	93	120	1.8×10^{35}	110

† $0 < \sqrt{s_{\gamma\gamma}} < \sqrt{s_{ee}}$

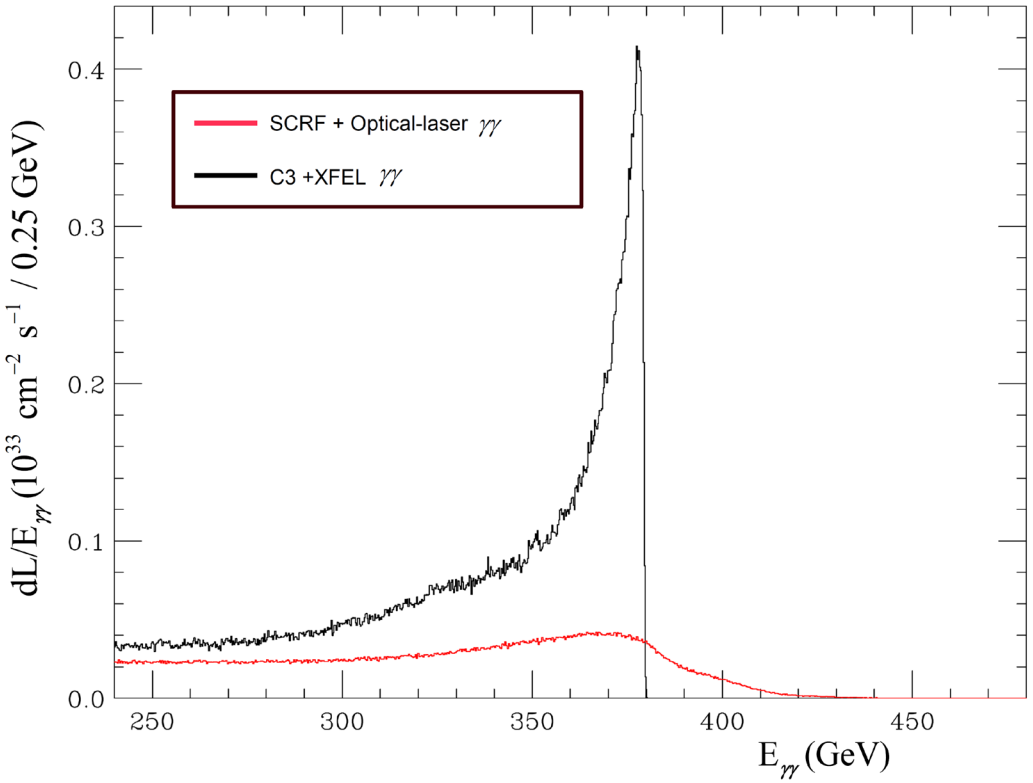

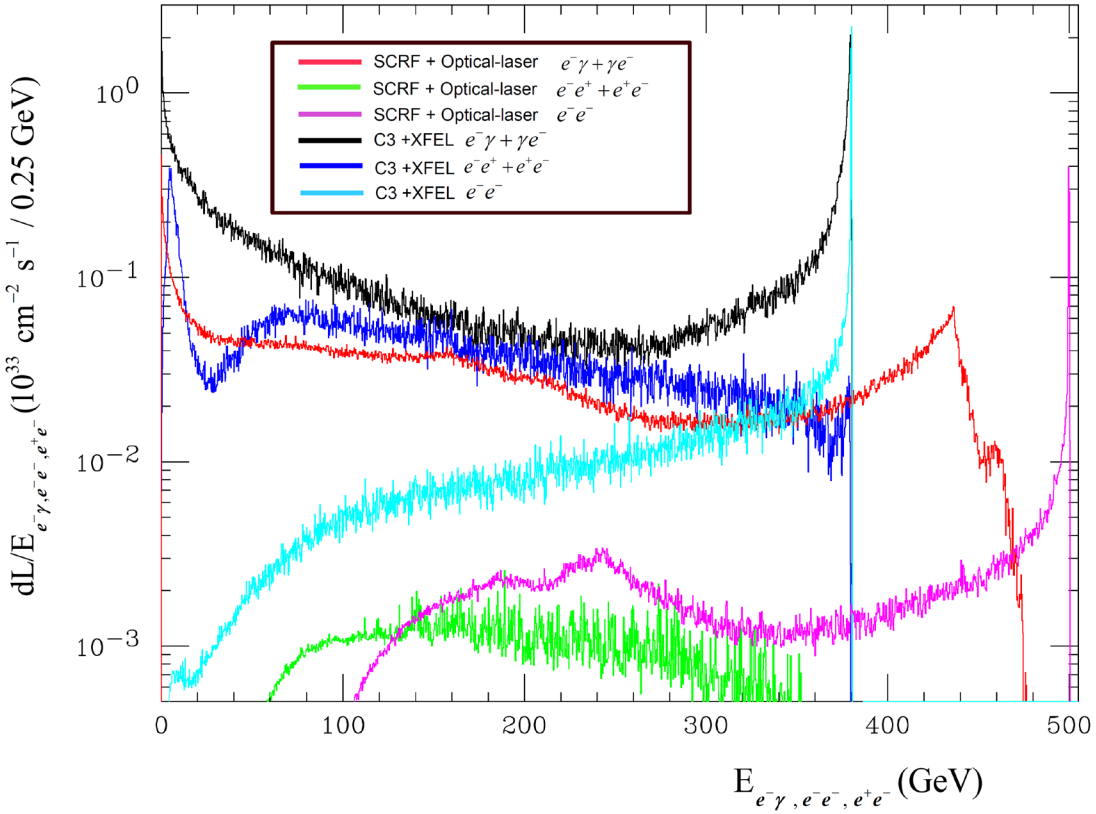

Comparison a bit unfair since XFEL collider requires much broader R&D program

Simulation of 15 TeV $\gamma\gamma$ Collider

Replace 62.5 GeV C^3 e- beam w/ 7500 GeV PWFA e- beam and simulate γγ Collisions using CAIN MC

Technology	PWFA	γγ PWFA
Aspect Ratio	Round	Round
CM Energy	15	15
Single beam energy (TeV)	7.5	7.5
Gamma	1.47E+07	1.4E+07
Emittance X (mm mrad)	0.1	0.12
Emittance Y (mm mrad)	0.1	0.12
Beta* X (m)	1.50E-04	0.30E-04
Beta* Y (m)	1.50E-04	0.30E-04
Sigma* X (nm)	1.01	0.48
Sigma* Y (nm)	1.01	0.48
N_bunch (num)	5.00E+09	5.00E+09
Freq (Hz)	7725	7725
Sigma Z (um)	5	5
Geometric Lumi (cm^2 s^1)	1.50E+36	6.58E+36

Start with x=4.8 because this was considered the typical γγ collider x value before this study was performed

x=4.8 adjust parameters to get ~ 100 % conversion w/ linear QED

$x = 4.8 \Rightarrow$ 9100 GeV e^- + 0.034 eV γ (λ=36 μm) $a_{\gamma FWHM} = 2.1$ mm $\sigma_{\gamma z} = 0.79$ mm $d_{cp} = 2.4$ mm

$\sigma_{ez} = 5\ \mu$m N_{e^-}=1 nC $\gamma\varepsilon_{x,y} = 120$ nm $2P_c\lambda_e = -0.9$ $E_{pulse} = 4400$ J

γ Energy Spectra

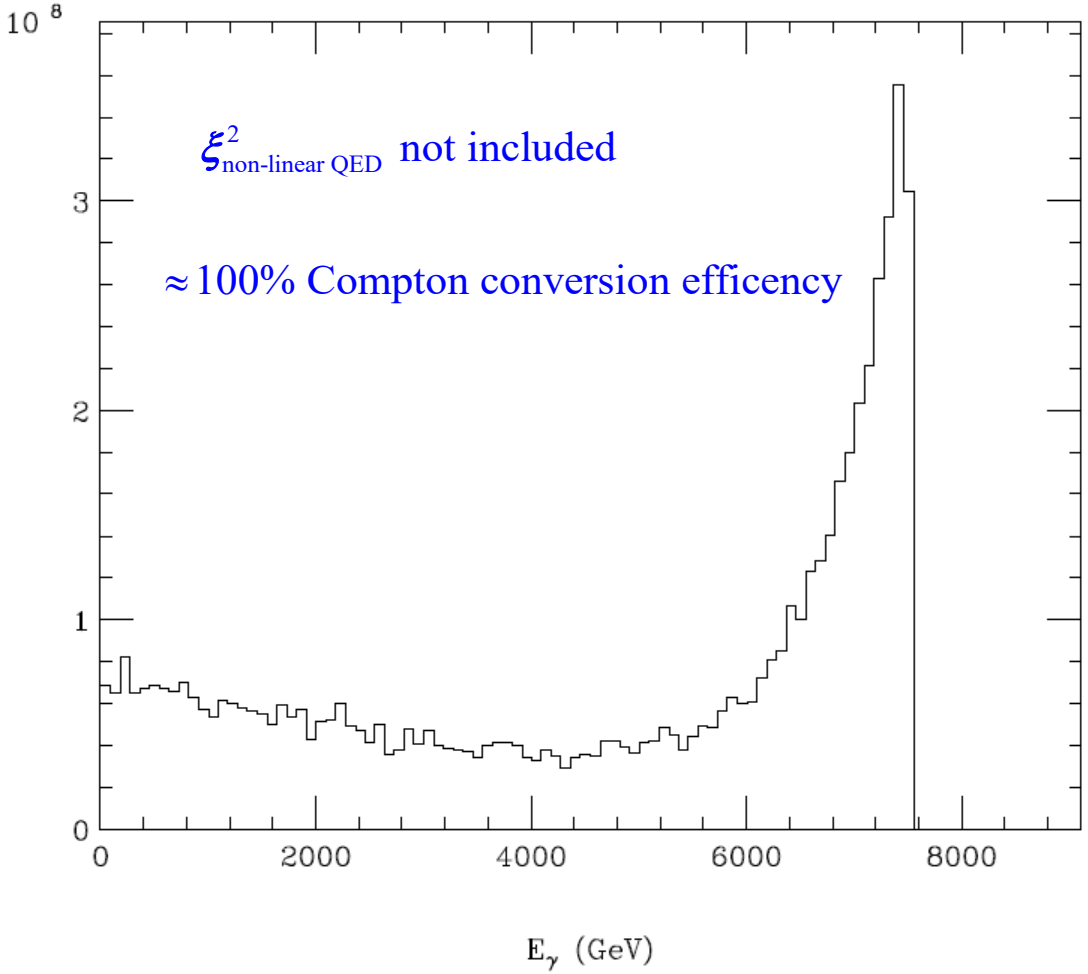

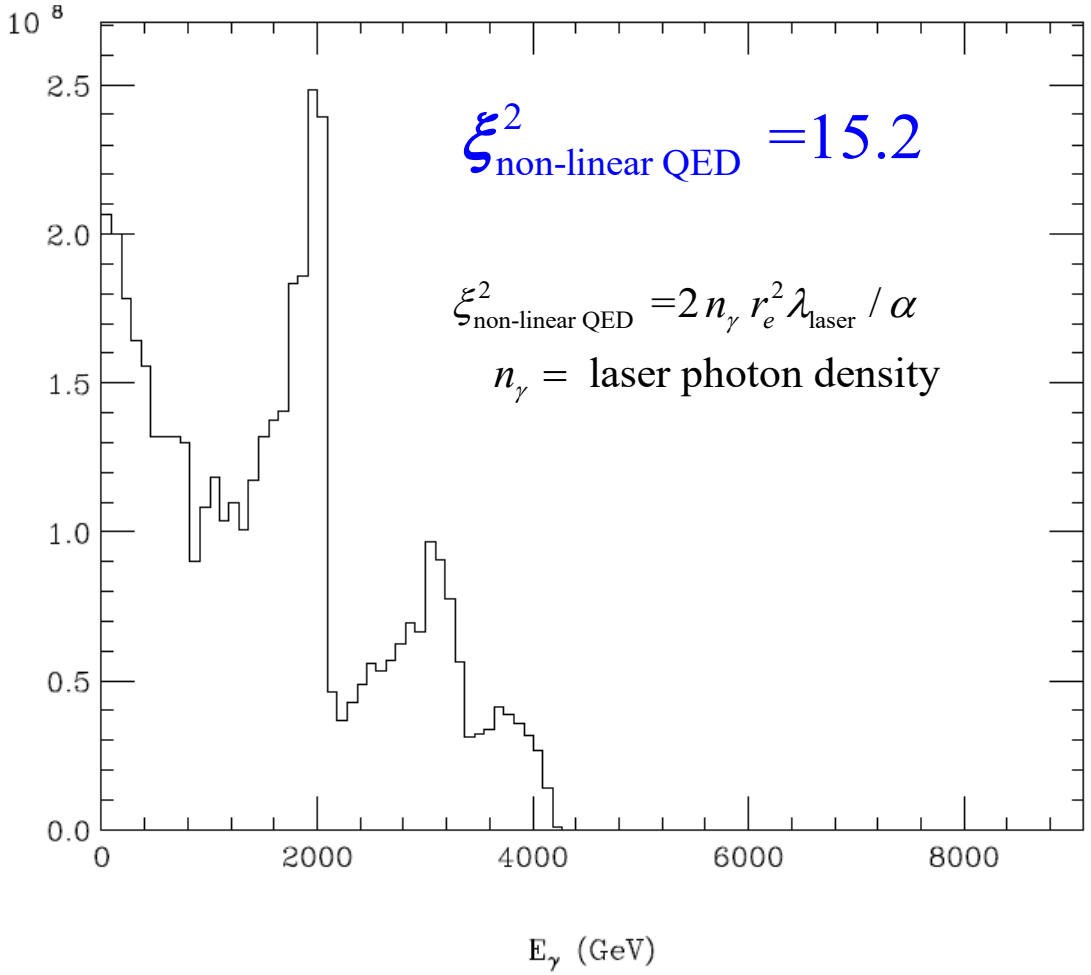

x=4.8 , parameters with ~ 100 % conversion w/ linear QED

$x = 4.8 \Rightarrow$ 9100 GeV e^- + 0.034 eV γ (λ=36 μm) $a_{\gamma FWHM} = 2.1$ mm $\sigma_{\gamma z} = 0.79$ mm $d_{cp} = 2.4$ mm

$\sigma_{ez} = 5$ μm N_{e^-}=1 nC $\gamma\varepsilon_{x,y} = 120$ nm $2P_c\lambda_e = -0.9$ $E_{pulse} = 4400$ J

$\gamma\gamma$ Luminosity Spectra

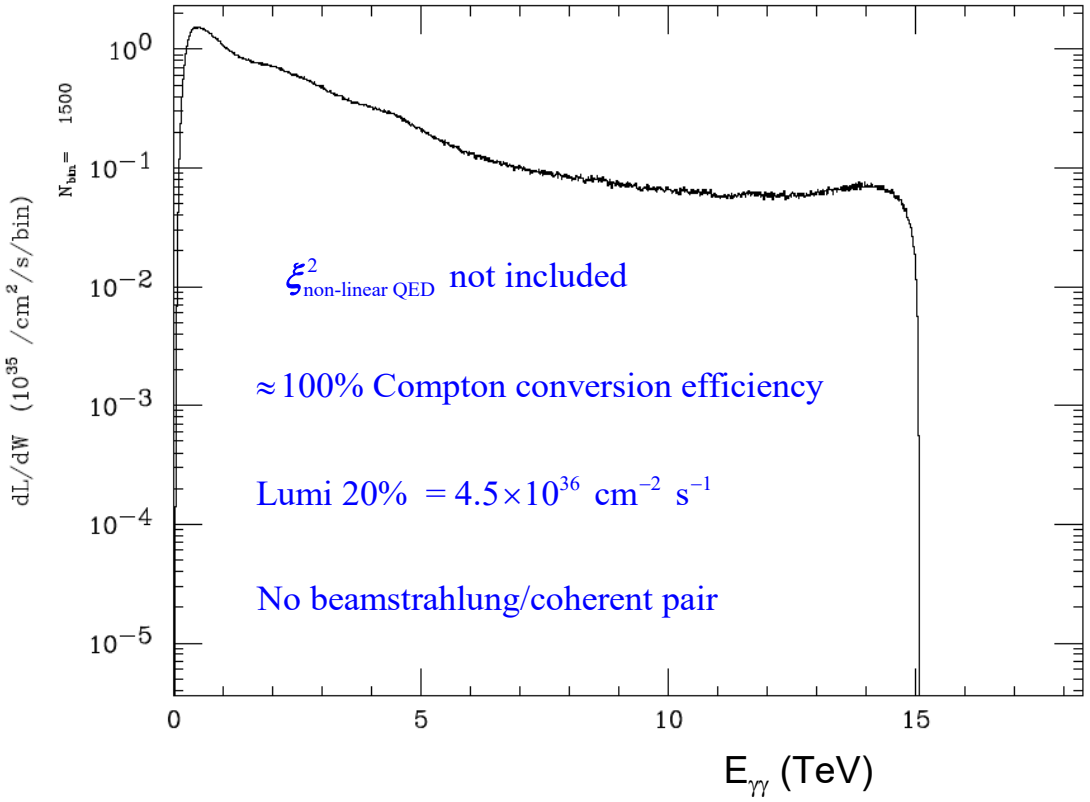

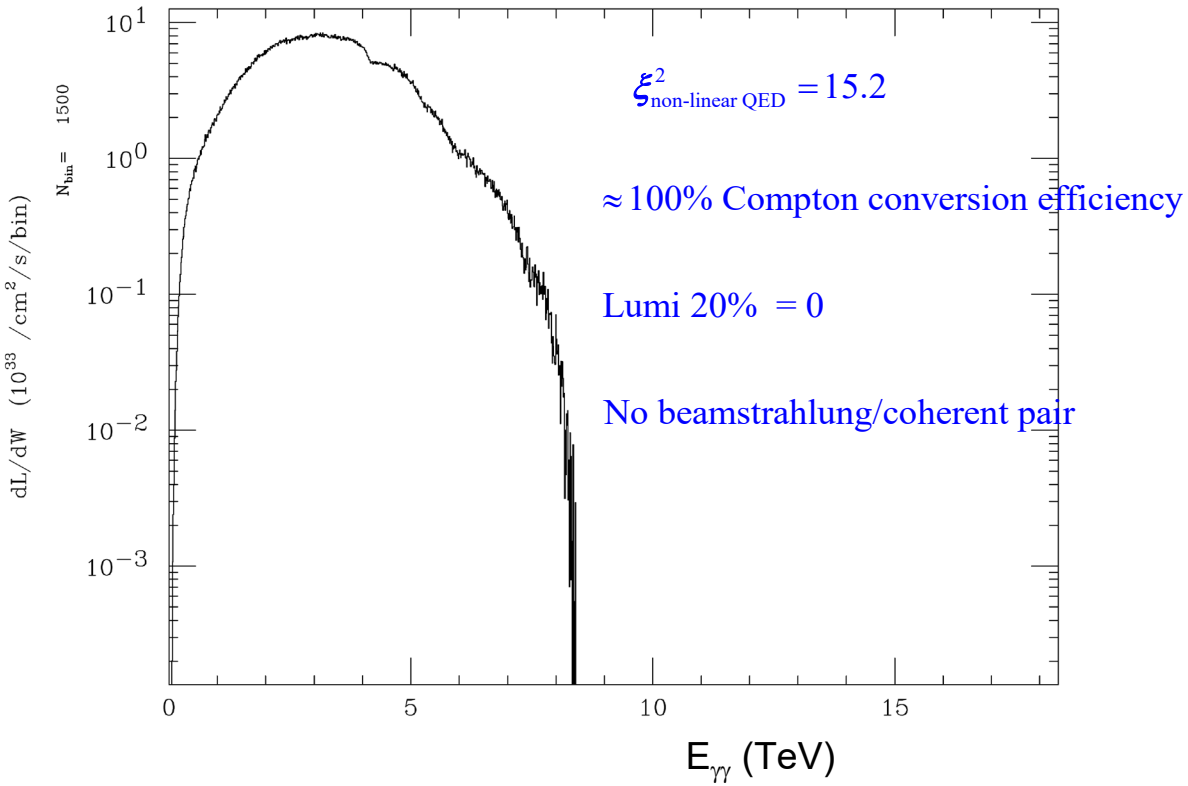

x=4.8 dial back E_{pulse} to get $\xi^2 < 1$

$x = 4.8 \Rightarrow$ 9100 GeV e^- + 0.034 eV γ (λ=36 μm) $a_{\gamma FWHM} = 2.1$ mm $\sigma_{\gamma z} = 0.79$ mm $d_{cp} = 2.4$ mm

$\sigma_{ez} = 5$ μm N_{e^-}=1 nC $\gamma\varepsilon_{x,y} = 120$ nm $2P_c\lambda_e = -0.9$ $E_{pulse} = 260$ J

γ Energy Spectra

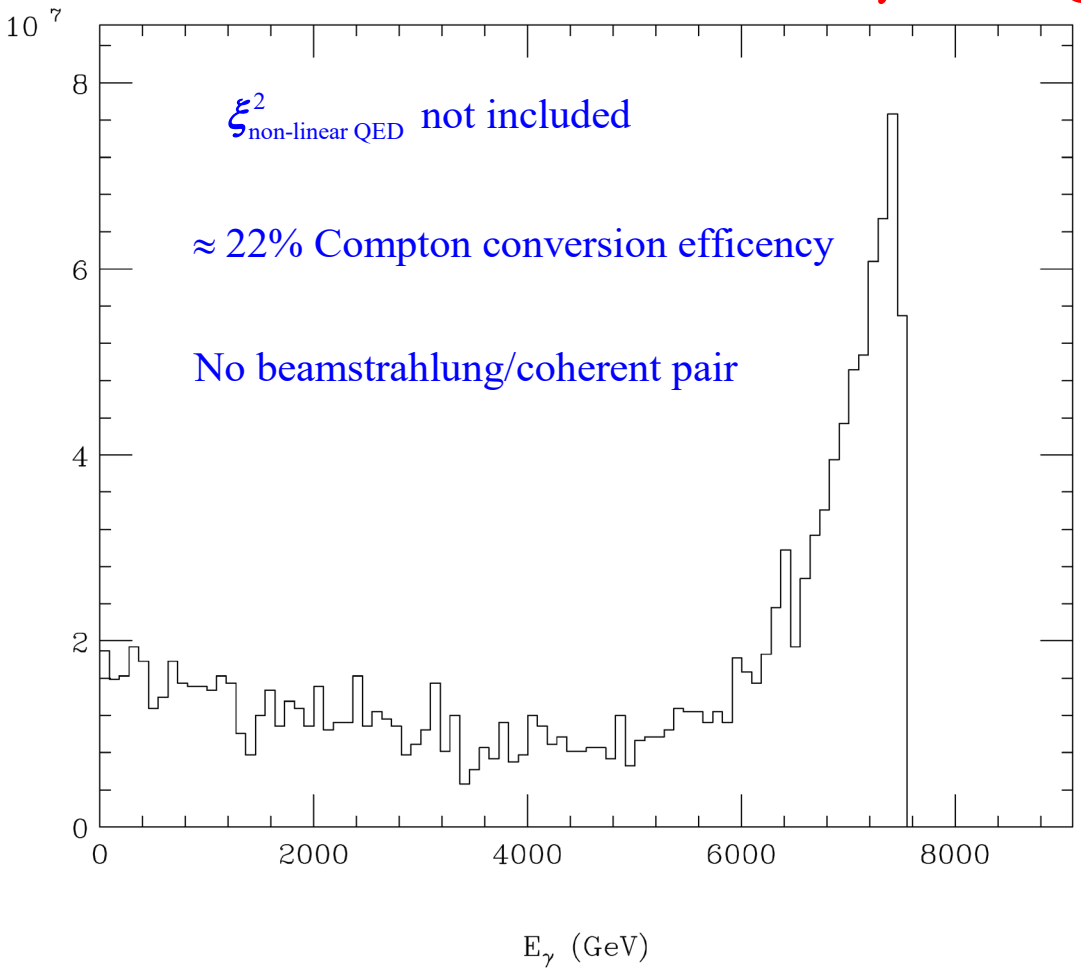

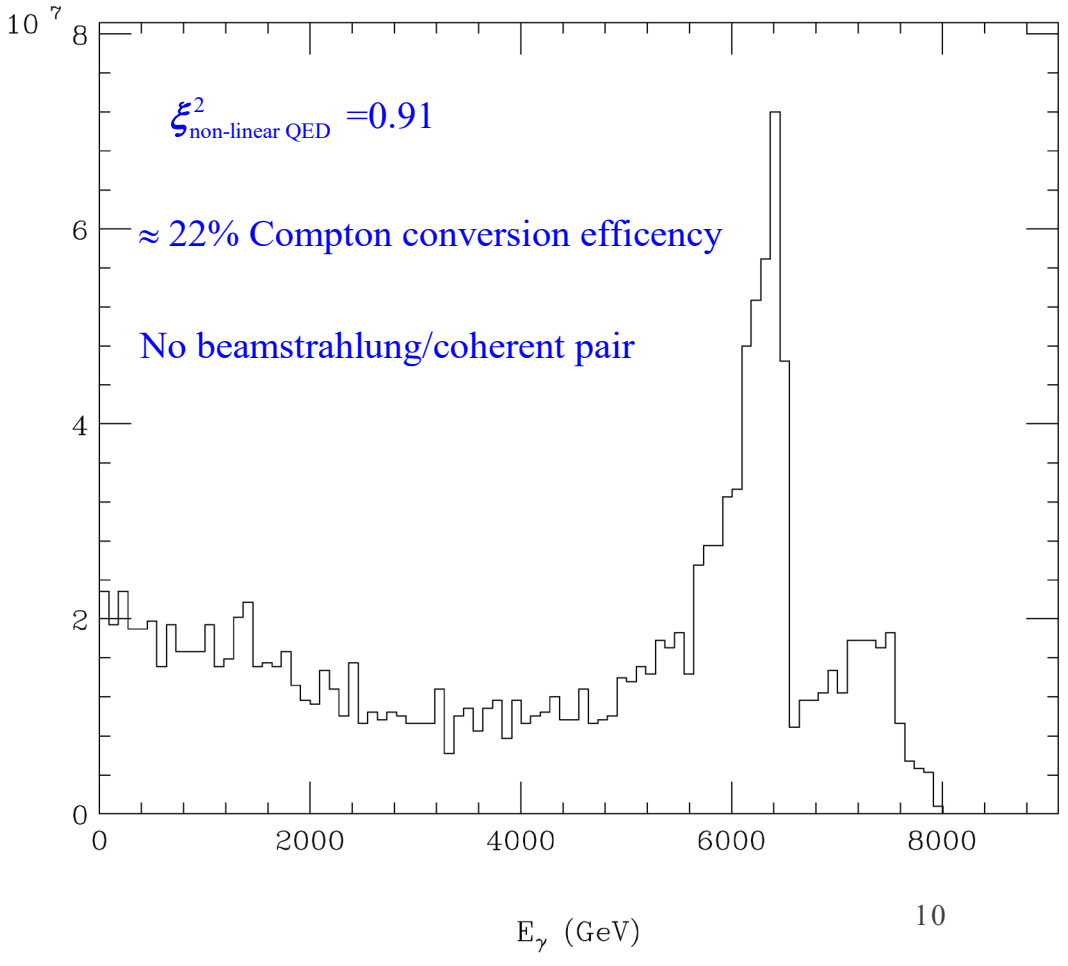

x=4.8 dial back E_{pulse} to get $\xi^2 < 1$

$x = 4.8 \Rightarrow$ 9100 GeV e^- + 0.034 eV γ (λ=36 μm) $a_{\gamma FWHM} = 2.1$ mm $\sigma_{\gamma z} = 0.79$ mm $d_{cp} = 2.4$ mm

$\sigma_{ez} = 5$ μm N_{e^-}=1 nC $\gamma\varepsilon_{x,y} = 120$ nm $2P_c\lambda_e = -0.9$ $E_{pulse} = 260$ J

$\gamma\gamma$ Luminosity Spectra

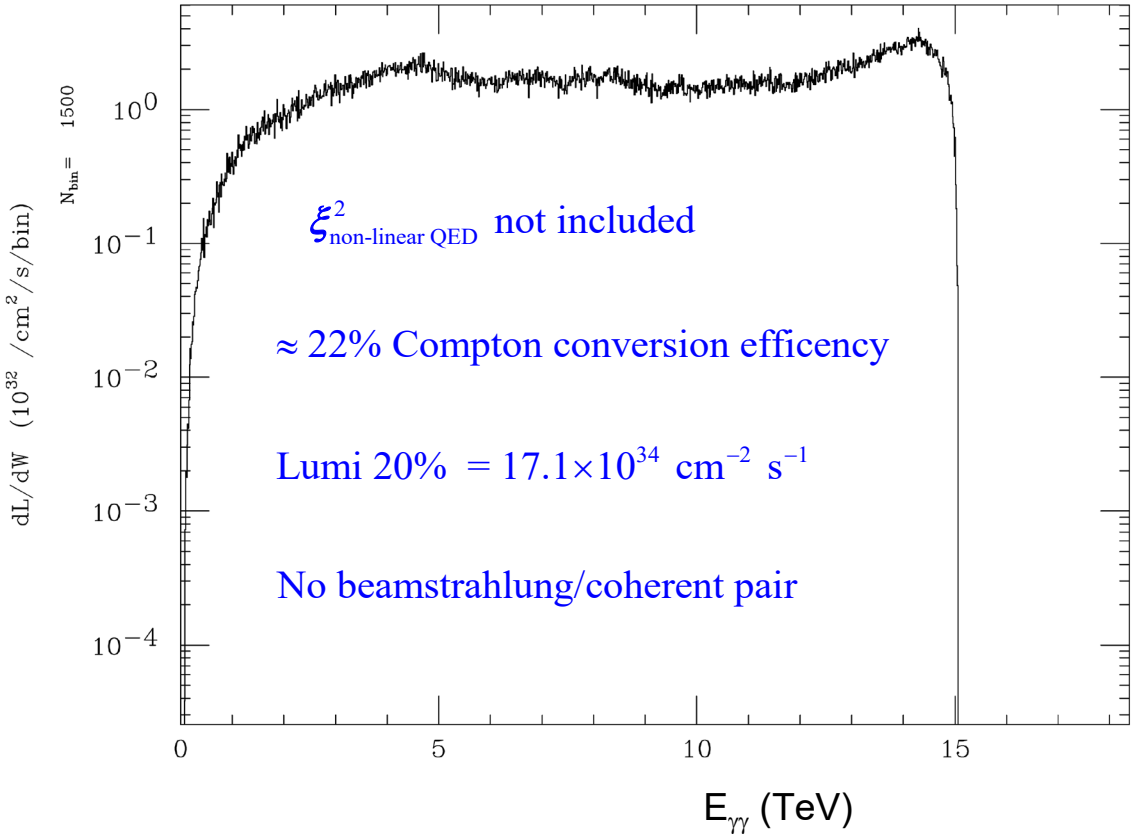

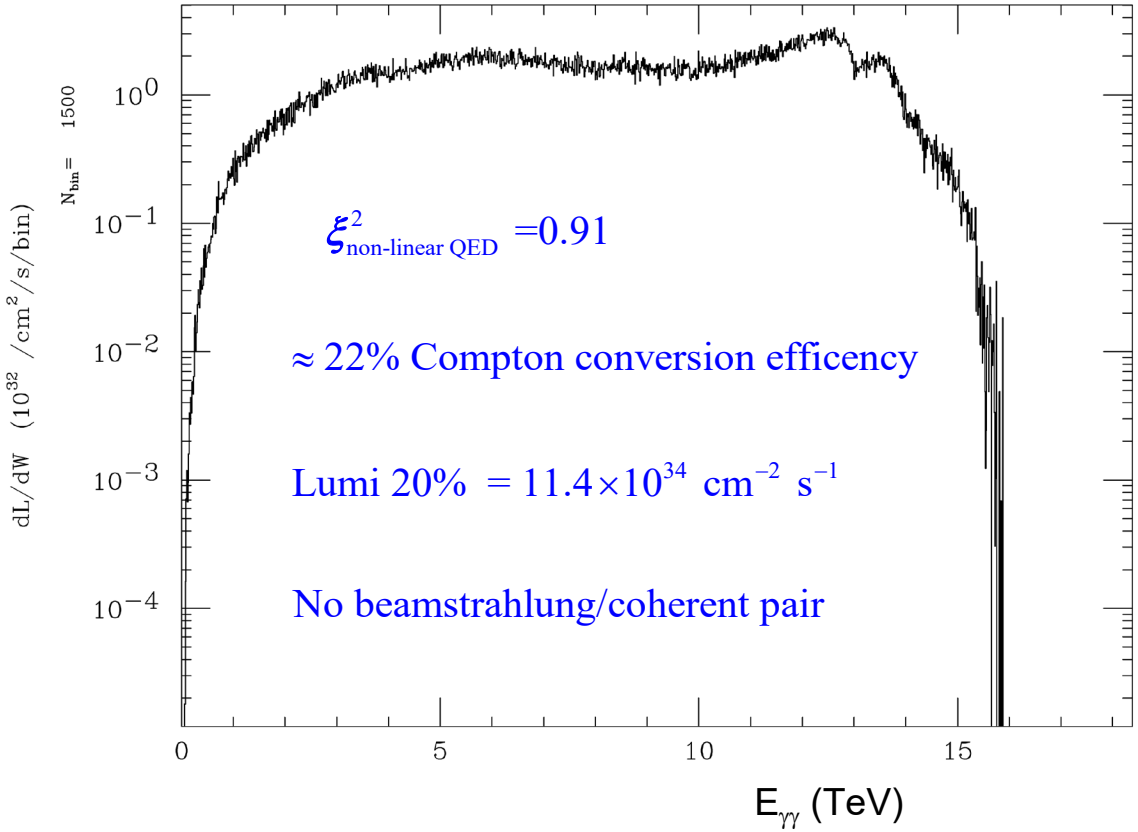

Try x=40 to get more of a peak in the spectrum

$x = 40 \Rightarrow$ 7875 GeV e^- + 0.33 eV γ (λ=3.7 μm) $a_{\gamma FWHM} = 0.24$ mm $\sigma_{\gamma z} = 270\ \mu$m $d_{cp} = 0.82$mm

$\sigma_{ez} = 5\ \mu$m $N_{e^-} = 5\times10^9$ $\gamma\varepsilon_{x,y} = 120$ nm $2P_c\lambda_e = -0.9$ $E_{pulse} = 590$ J

$\gamma\gamma$ Luminosity Spectrum

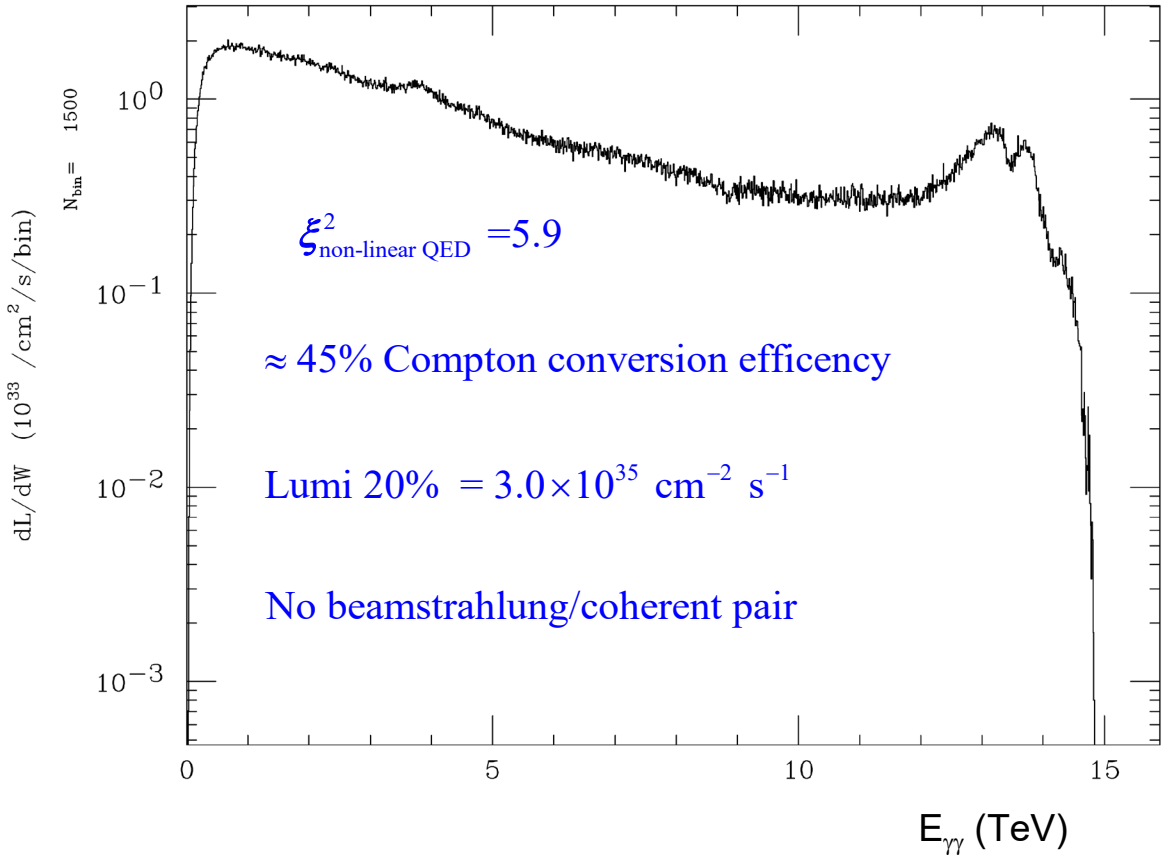

15 TeV and x=40 Turn on coherent processes

$x = 40 \Rightarrow$ 7875 GeV $e^- + 0.33$ eV γ (λ=3.7 μm) $a_{\gamma FWHM} = 0.24$ mm $\sigma_{\gamma z} = 270$ μm $d_{cp} = 0.82$mm

$\sigma_{ez} = 5$ μm $N_{e^-} = 5\times10^9$ $\gamma\varepsilon_{x,y} = 120$ nm $2P_c\lambda_e = -0.9$ $E_{pulse} = 590$ J

Halfway through the collision CAIN complains:

(SUBR.COHPAR) Algorithm of coherent pair generation wrong.
Call the programmer prob,pmaxco= 8.309E-01 8.000E-01

Solution:

number of macro particles produced per coherent beamstrahlung photon = 1 → 0.01
number of pairs of macro particles produced per coherent e+e- pair = 1 → 0.0001
number of macro particles produced per incoherent particle = 1 → 0.01

15 TeV and x=40 Turn on coherent processes

$x = 40 \Rightarrow$ 7875 GeV $e^- + 0.33$ eV γ (λ=3.7 μm) $a_{\gamma FWHM} = 0.24$ mm $\sigma_{\gamma z} = 270\ \mu$m $d_{cp} = 0.82$mm

$\sigma_{ez} = 5\ \mu$m $N_{e^-} = 5\times10^9$ $\gamma\varepsilon_{x,y} = 120$ nm $2P_c\lambda_e = -0.9$ $E_{pulse} = 590$ J

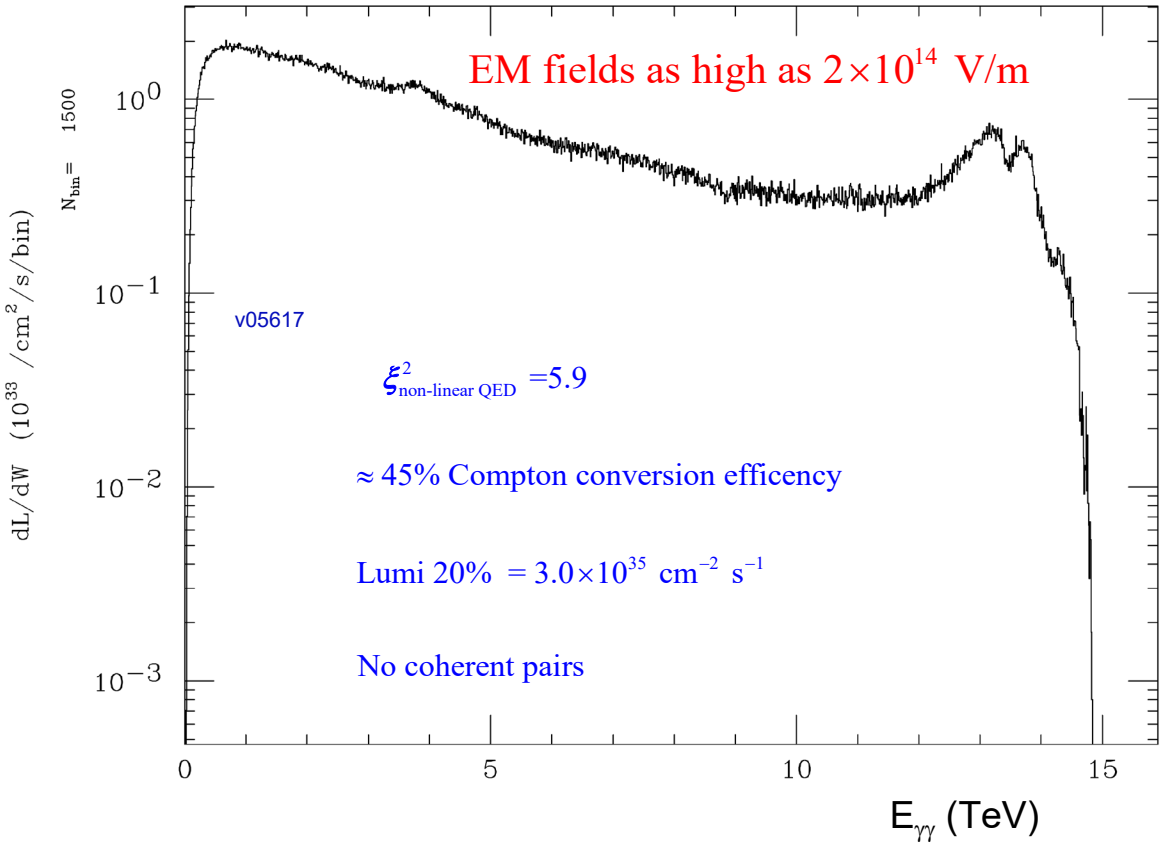

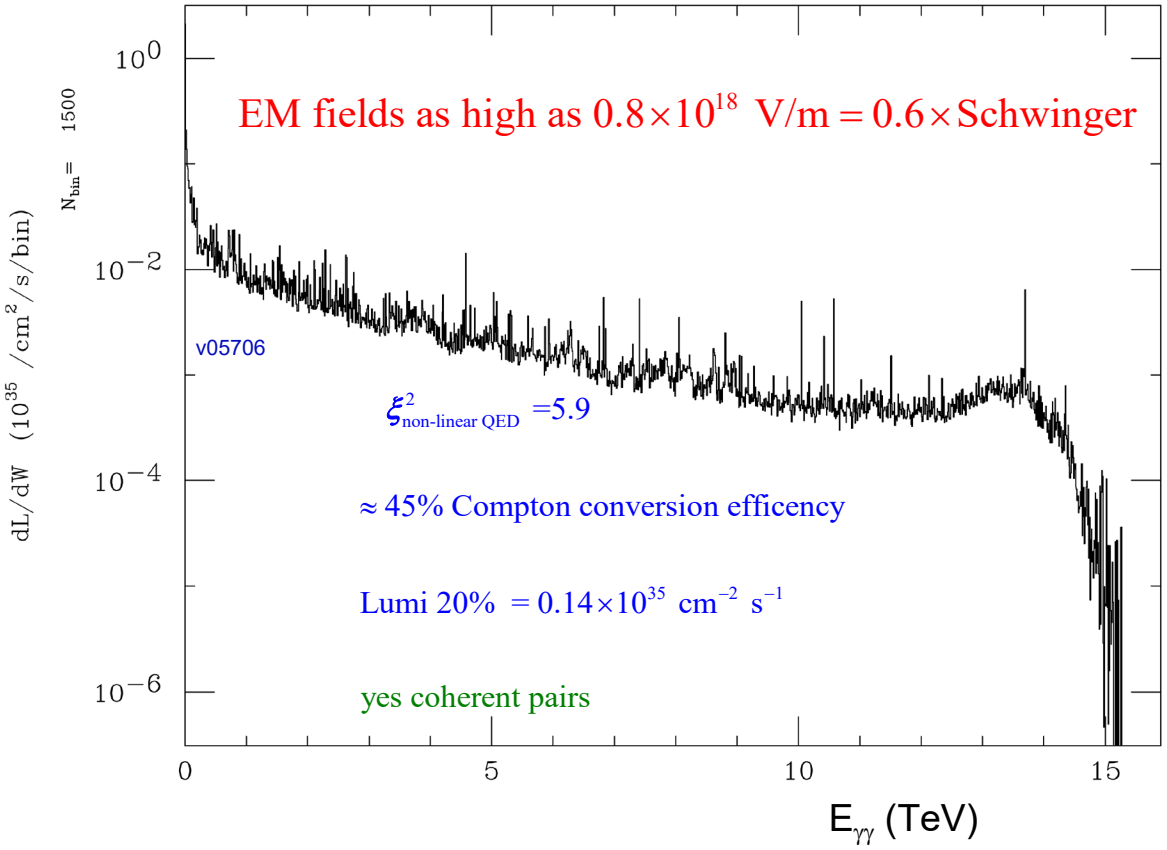

Coherent pair production eats up the 7.5 TeV photons and produces many e+ that pinch the e- beam leading to higher fields and even more coherent pair production.

$e^-\gamma$ collisions at $E_{e\gamma}$=140 GeV I.P. geometric e^- σ_x,σ_y=5.1 nm

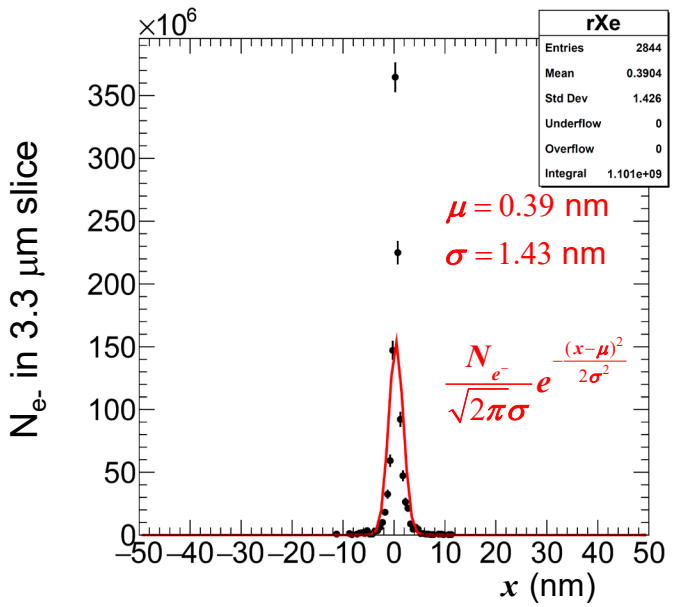

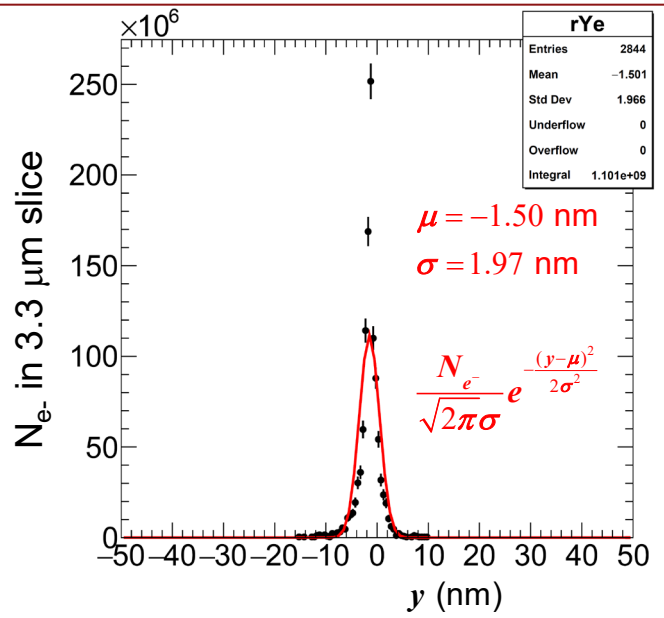

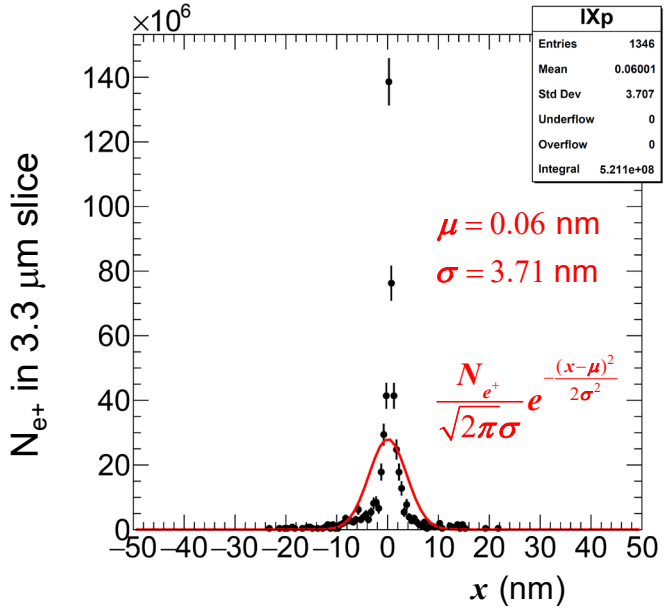

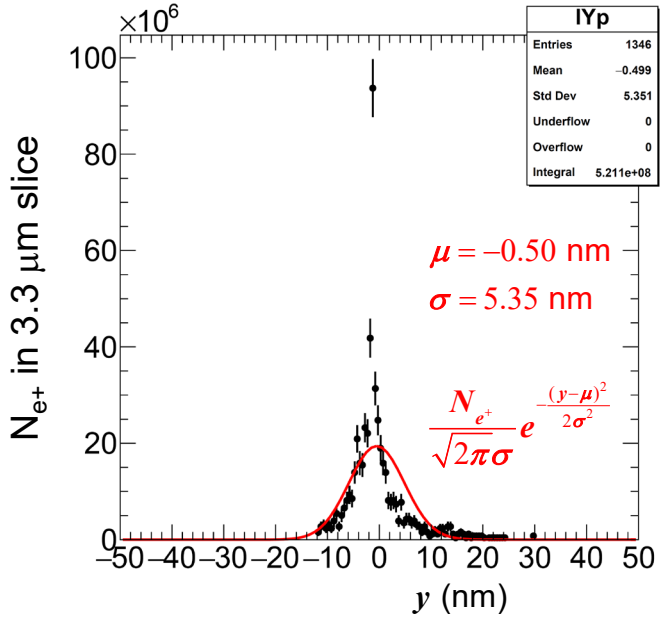

During the collision, the e^+ from coherent e^+e^- production are focused by the EM field of the oncoming e^- beam. This leads to focusing (pinching) of the e^- beam.

This pinching creates very high fields which leads to even more coherent pair production and even higher fields.

x=1.2x10^5 (1 keV γ) not affected as much by coherent processes

$x = 1.2\times10^5 \Rightarrow$ 7500 GeV e^- + 1 keV γ (λ=1.2 nm)

$a_{\gamma FWHM} = 70$ mm $\sigma_{\gamma z} = 5\ \mu$m $d_{cp} = 15\ \mu$m

$\sigma_{ez} = 5\ \mu$m $N_{e^-} = 6\times10^9$ $\gamma\varepsilon_{x,y} = 120$ nm

$2P_c\lambda_e = +0.9$ $E_{pulse} = 0.72$ J

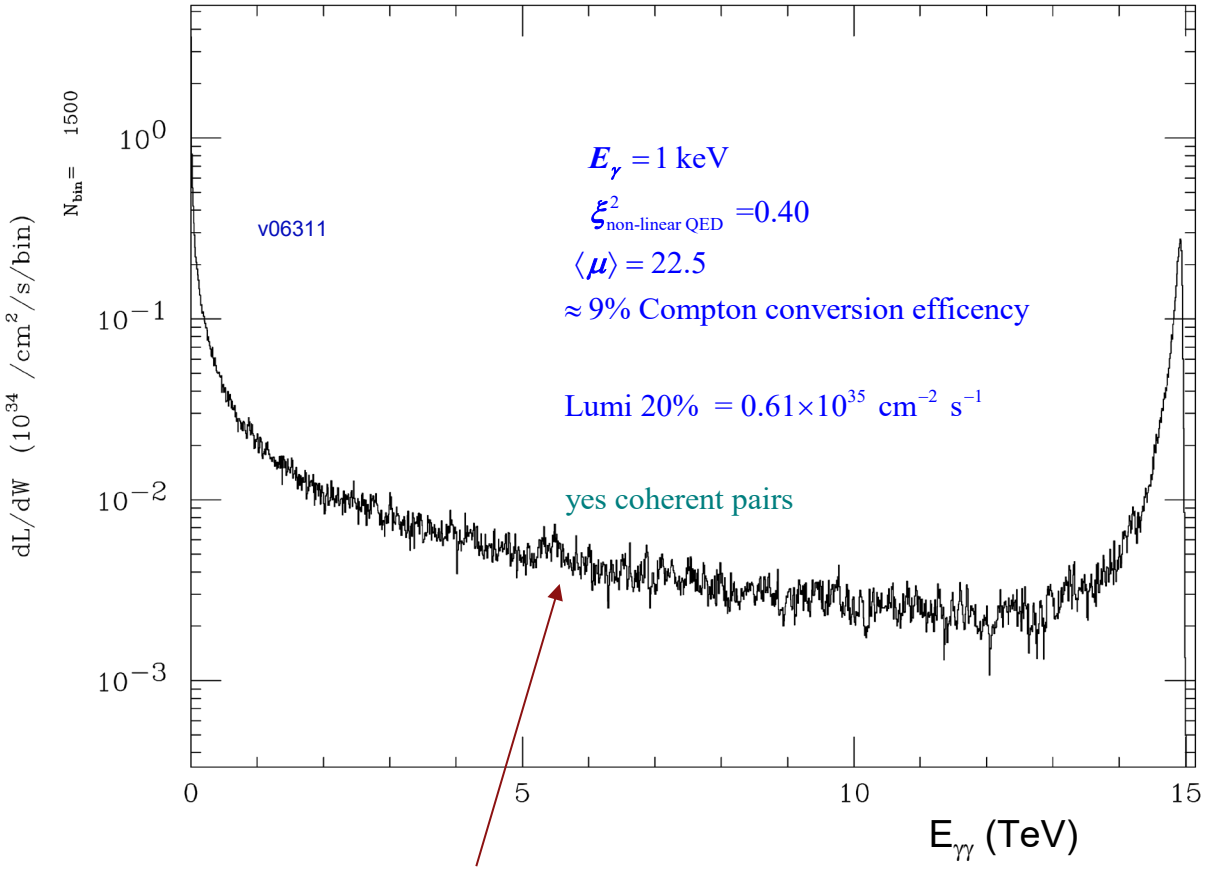

$x = 40 \Rightarrow$ 7875 GeV e^- + 0.33 eV γ (λ=3.7 μm)

$a_{\gamma FWHM} = 0.24$ mm $\sigma_{\gamma z} = 270\ \mu$m $d_{cp} = 0.82$mm

$\sigma_{ez} = 5\ \mu$m $N_{e^-} = 5\times10^9$ $\gamma\varepsilon_{x,y} = 120$ nm

$2P_c\lambda_e = -0.9$ $E_{pulse} = 590$ J

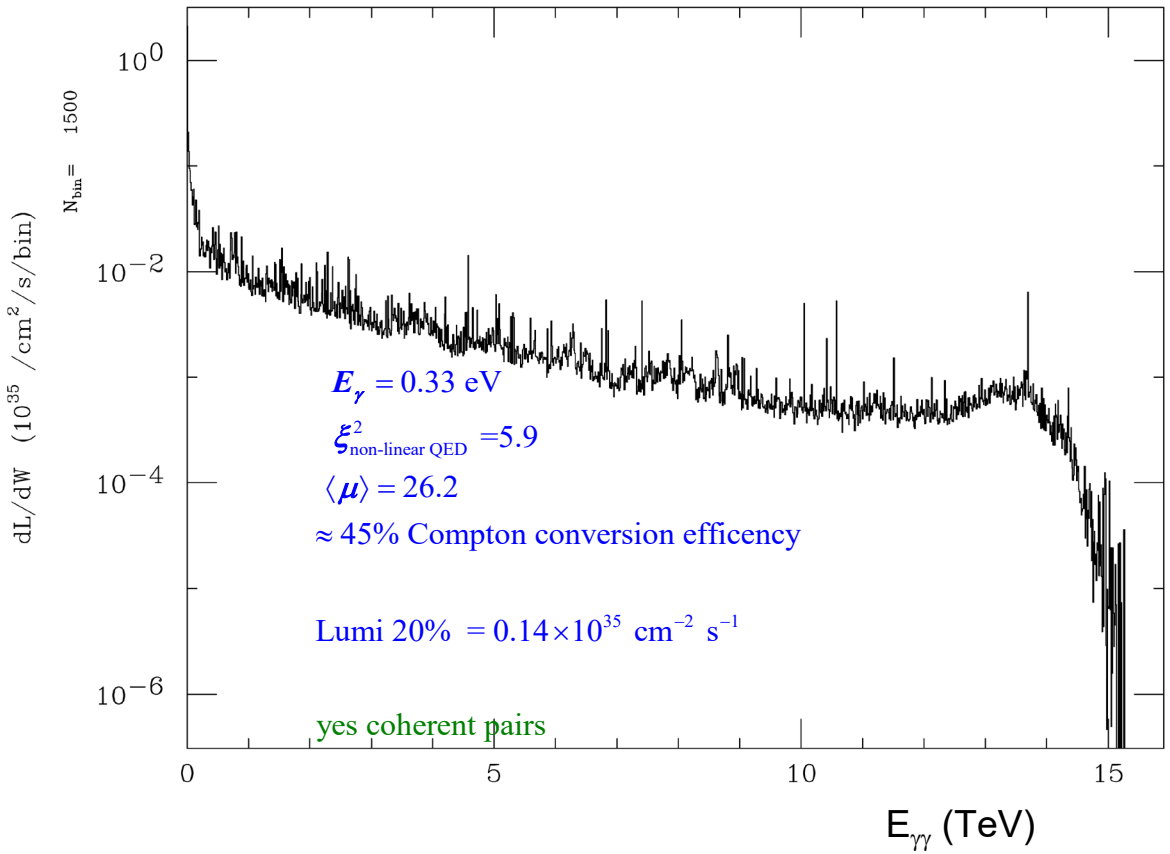

e^- from Compton IP have much reduced energy due to multiple trident $e^-\gamma \rightarrow e^-e^+e^-$. EM fields are 3 orders of magnitude smaller.

$\gamma\gamma \to N \times e^+e^-$, $e^-\gamma \to e^- + N \times e^+e^-$, $N = 2,3,\ \ldots$

$x = 1.2\times10^5 \Rightarrow$ 7500 GeV e^- + 1 keV γ (λ=1.2 nm) $a_{\gamma FWHM} = 70$ mm $\sigma_{\gamma z} = 5\ \mu$m $d_{cp} = 15\ \mu$m

$\sigma_{ez} = 5\ \mu$m N_{e^-}=1 nC $\gamma\varepsilon_{x,y} = 120$ nm $2P_c\lambda_e = +0.9$ $E_{pulse} = 0.72$ J

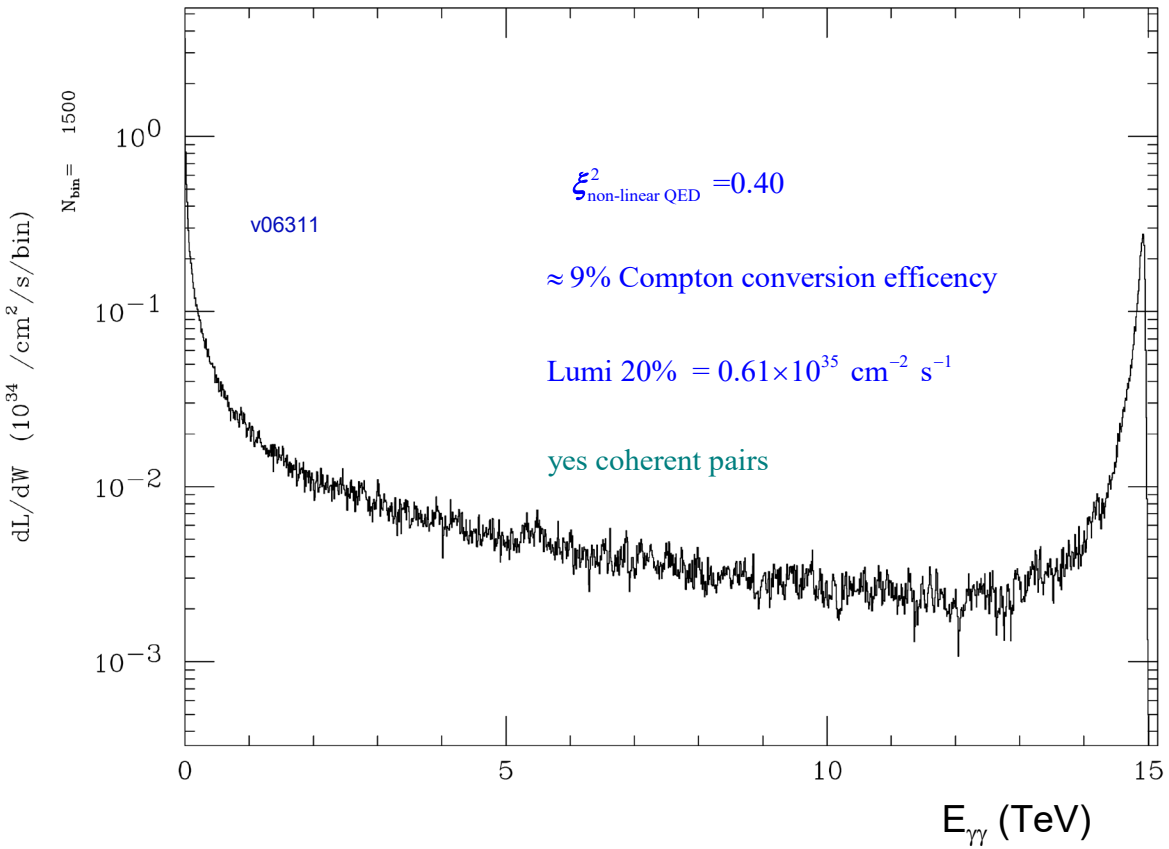

$\gamma\gamma \to N \times e^+e^-$, $e^-\gamma \to e^- + N \times e^+e^-$, $N = 2,3,\ \ldots$ are not simulated by CAIN.

$N \geq 2$ cross sections relatively small for $x \leq 1000$, but what about at $x \sim 10^5$?

Cross section Table for 1 keV laser γ calculated using Tree-level MC Integration:

Note: processes colored red are included in the CAIN MC

process	E_{e^-} (GeV)/x = 62.6 / 1000	E_{e^-} (GeV)/x = 5000 / 80,000	E_{e^-} (GeV)/x = 7500 / 120,000
$\gamma\gamma \to e^+e^-$	$2.16\times10^{12}\pm0.03\%$	$2.68\times10^{10}\pm0.07\%$	
$\gamma\gamma \to e^+e^-e^+e^-$	$3.26\times10^{9}\pm0.27\%$	$5.70\times10^{9}\pm0.92\%$	
$\gamma\gamma \to e^+e^-e^+e^-e^+e^-$		$2.33\times10^{4}\pm11.9\%$	
$e^-\gamma \to e^-e^+e^-$	$8.22\times10^{12}\pm0.22\%$	$9.55\times10^{11}\pm13.4\%$	$4.61\times10^{10}\pm30.4\%$
$e^-\gamma \to e^-e^+e^-e^+e^-$	$1.63\times10^{7}\pm0.78\%$	$5.68\times10^{6}\pm21.1\%$	$7.47\times10^{5}\pm17.4\%$

The relative MC integration statistical error increases for $x \sim 10^5$ but it is good enough to demonstrate that the $N = 1$ processes still dominate at $x \sim 10^5$ and therefore the current CAIN MC is valid.

Compare 15 and 10 TeV

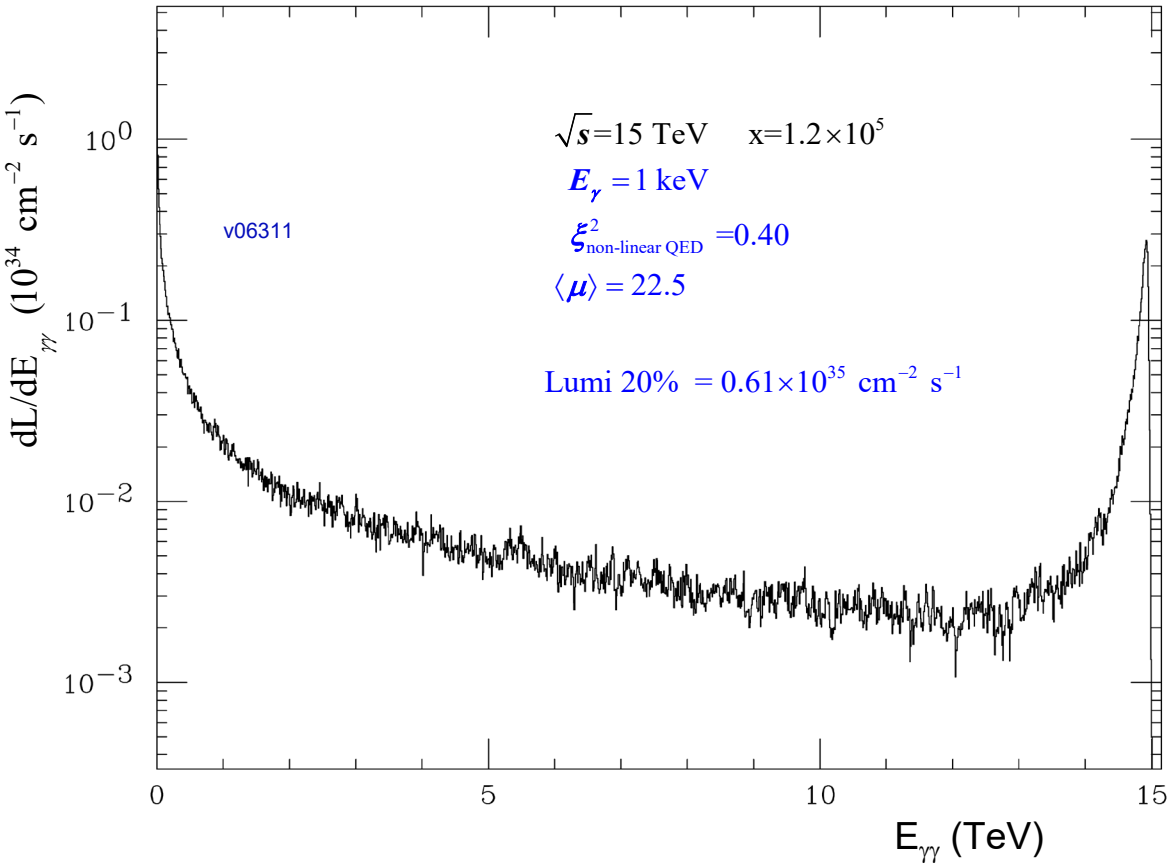

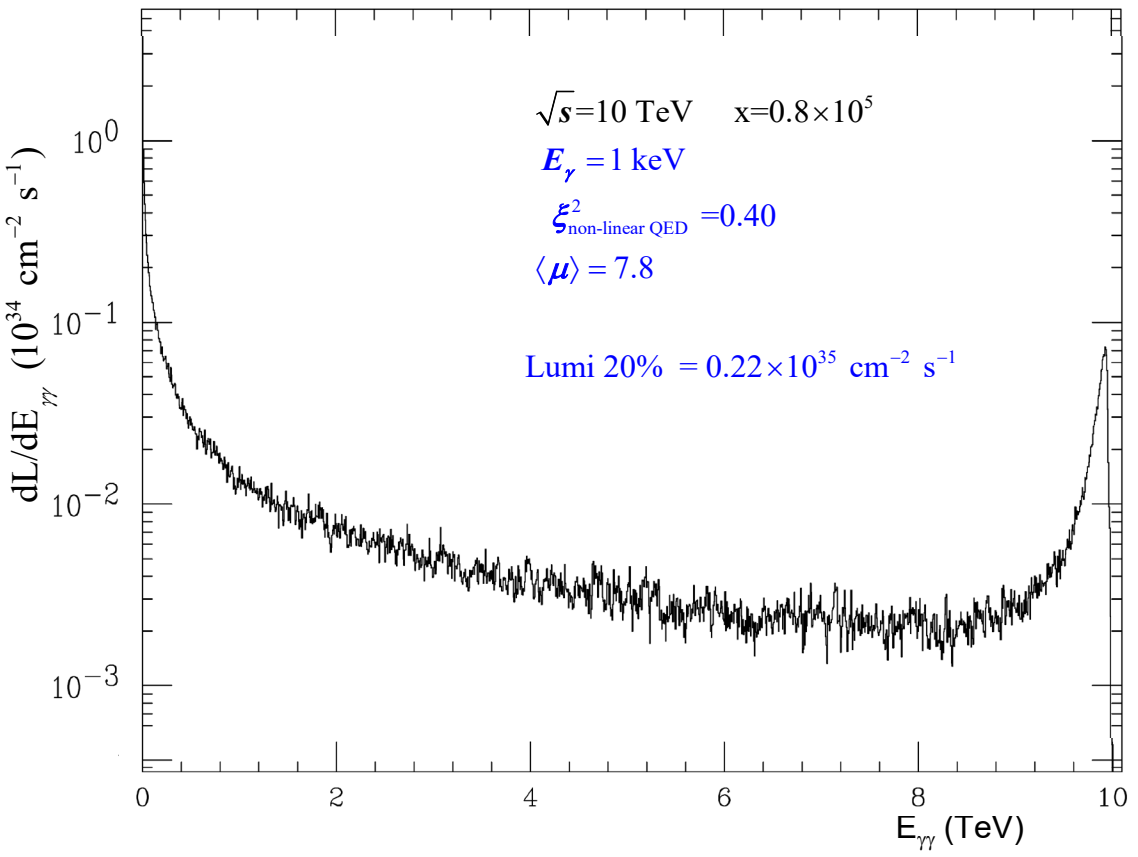

10 TeV $\gamma\gamma$ Luminosity: Compton vs e^-e^- Collider

Compton Collider

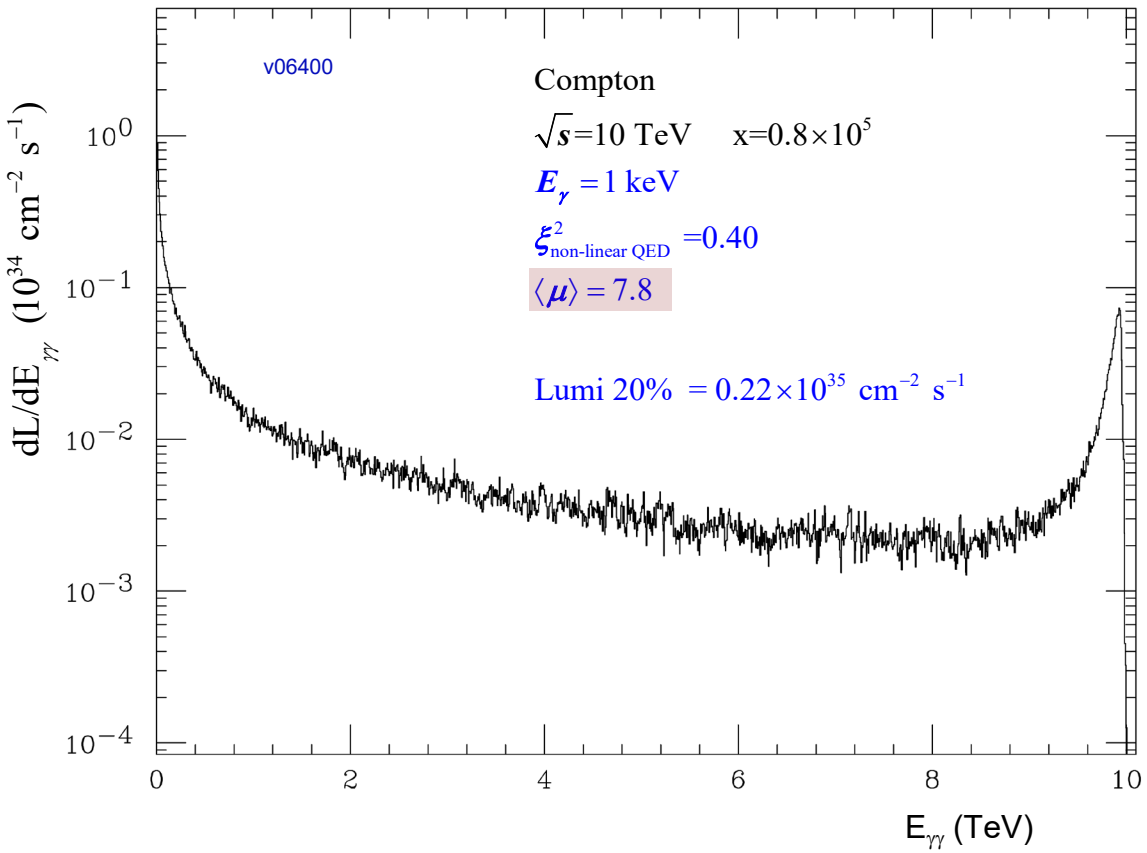

e^-e^- Collider

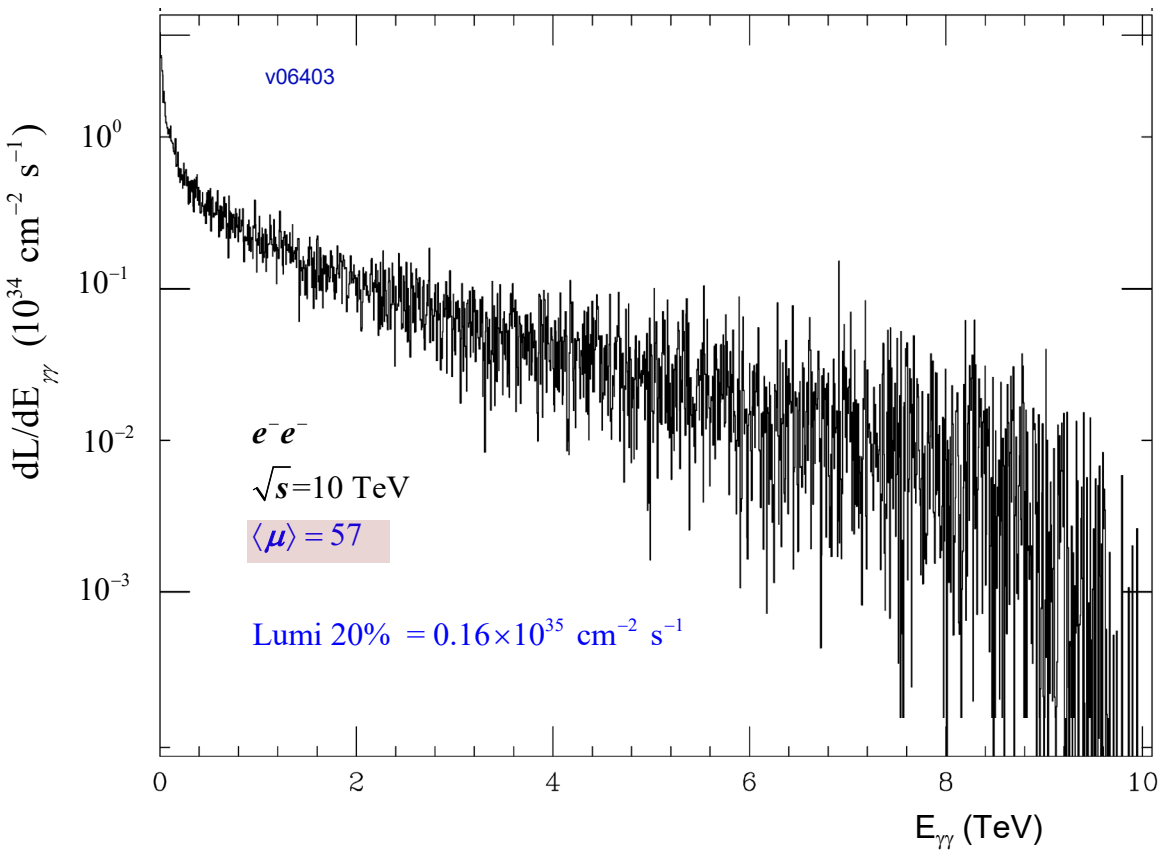

The top 20% Compton $\gamma\gamma$ Lumi is only 38% larger than the top 20% from e^-e^- beamstrahlung.

But at $\langle\mu\rangle = 57$ the e^-e^- Collider pileup is over seven times that of Compton, and the same as Run3 LHC.

10 TeV Compton Collider $\gamma\gamma$ $e^-\gamma$ γe^- e^-e^- e^+e^- e^-e^+

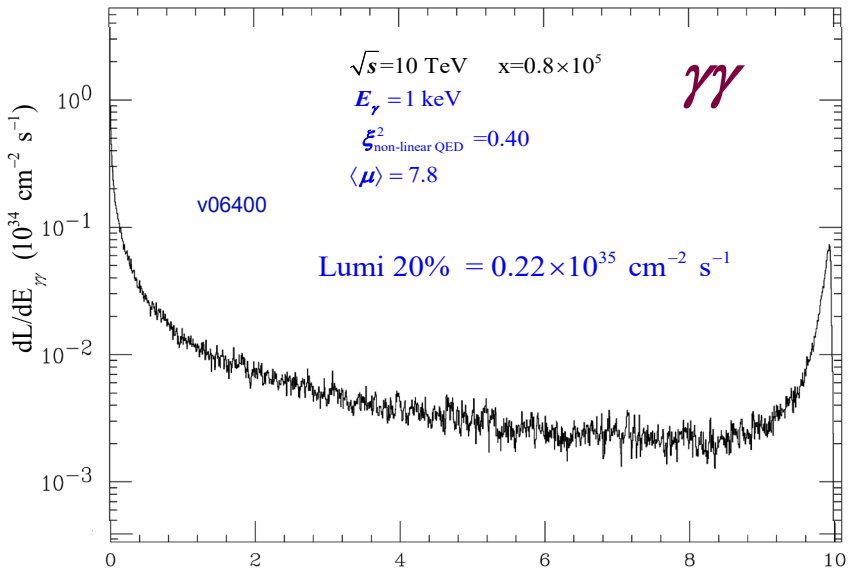

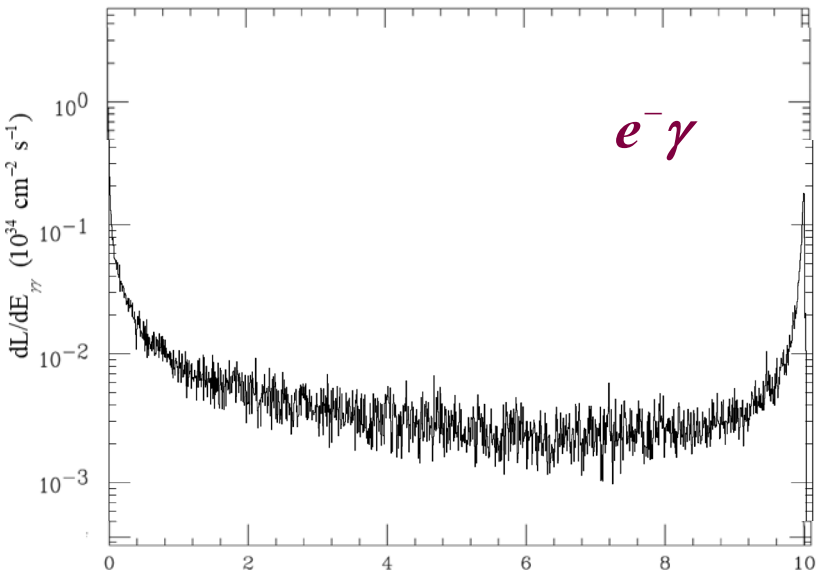

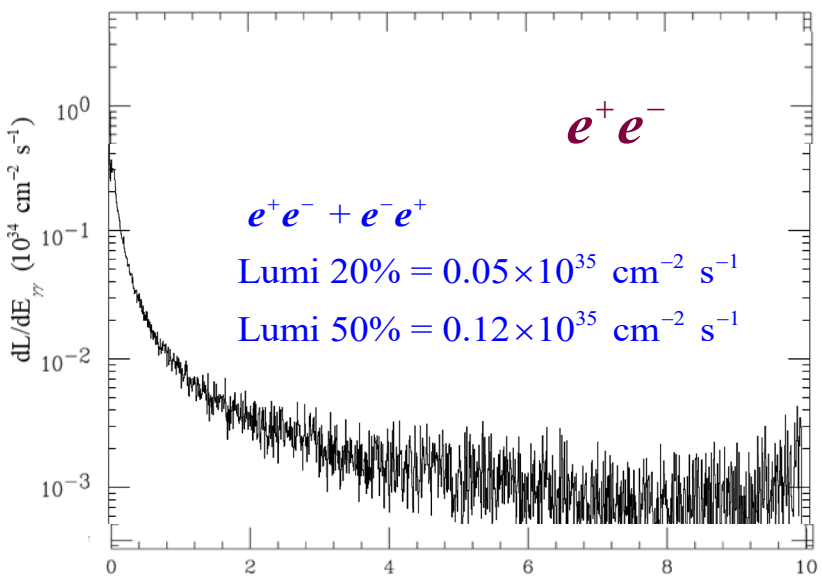

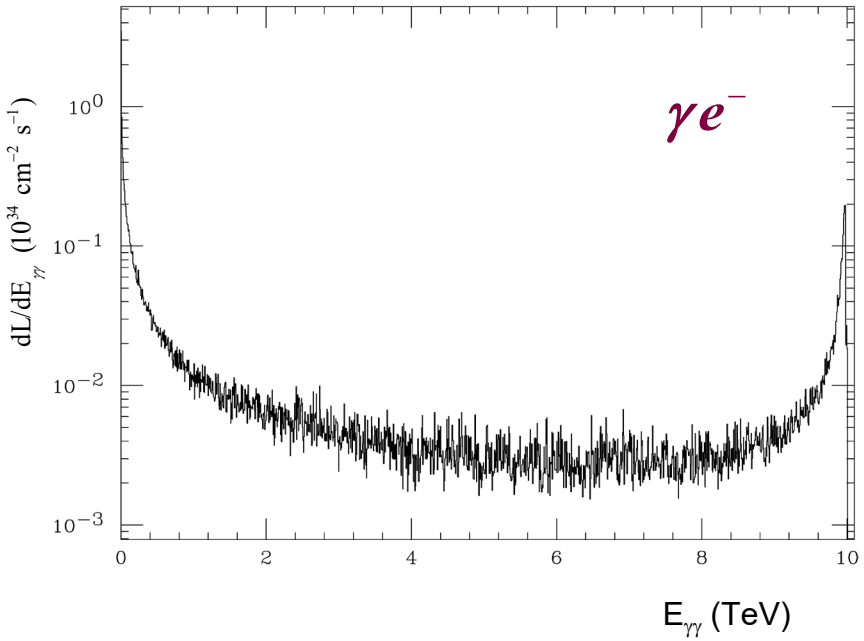

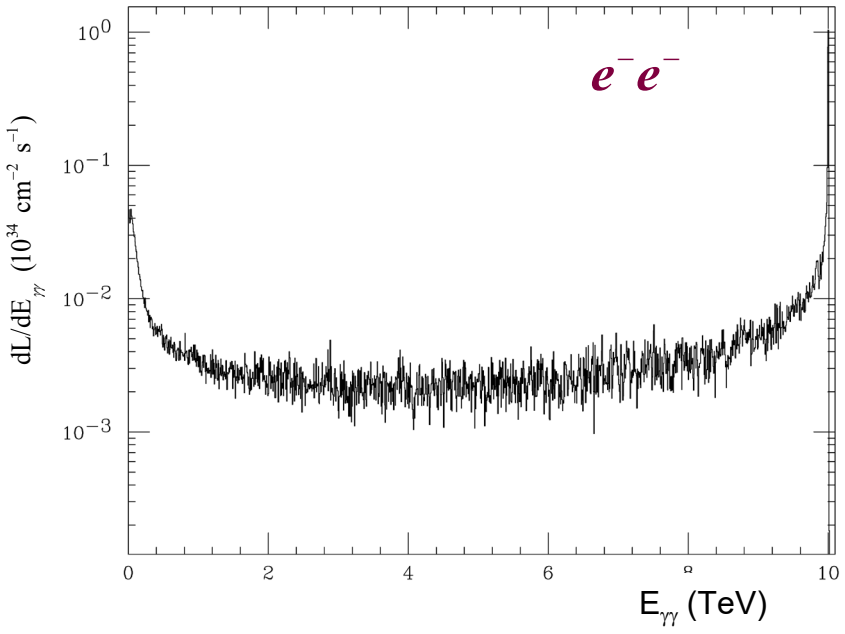

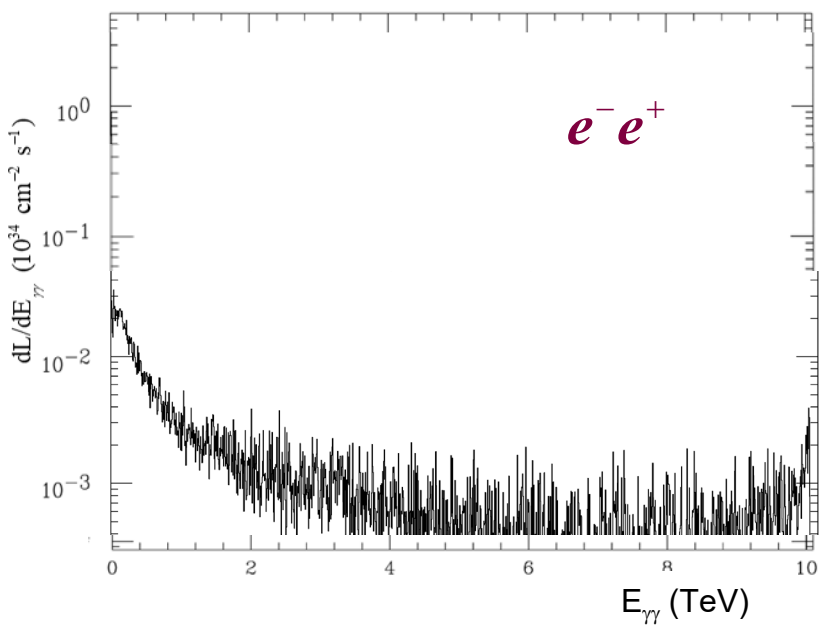

10 TeV e^-e^- Collider $\gamma\gamma$ $e^-\gamma$ γe^- e^-e^-

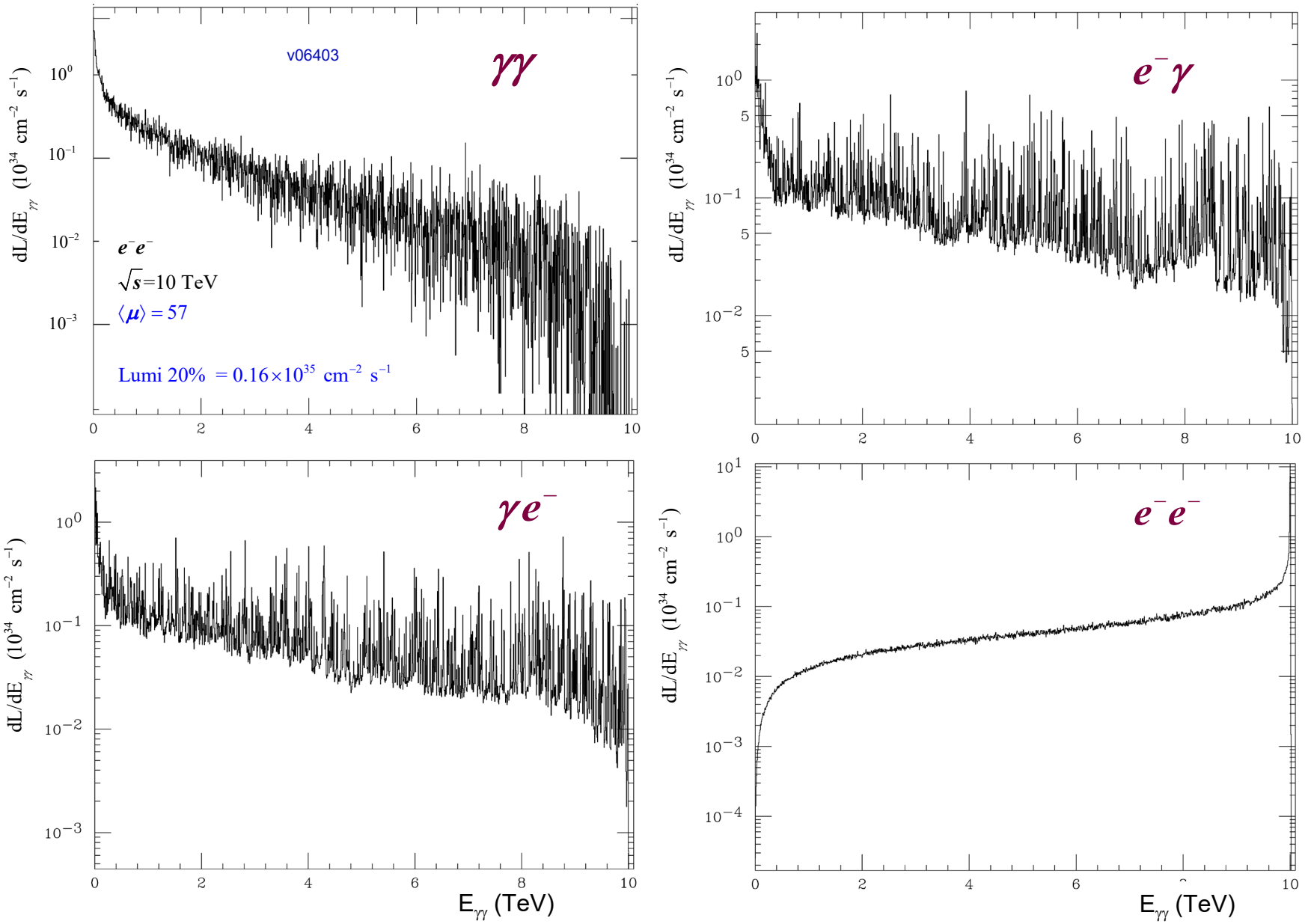

XCC Collider Accelerator Challenges

Electron beam:

- Polarized low emittance (120 nm) e^- injector is baseline XCC
  but damping ring would also work
- Focusing of round e^- beams to $\sigma_{x,y} = 5.5$ nm $(\beta_{x,y} = 0.03$ mm, $L_{geo} = 10^{35}$ cm^{-2}s$^{-1})$
  or asymmteric e^- beams if damping ring is used.

XFEL beam and Compton IP:

- Production of 1 keV γ XFEL with 700 mJ/pulse
- Focusing of 1 keV , 700 mJ/pulse XFEL beam to 70 nm FWHM waist
- XFEL and e^- beamline layouts around the IP
- Timing and position stability of the XFEL laser beam and e^- beam at Compton IP.

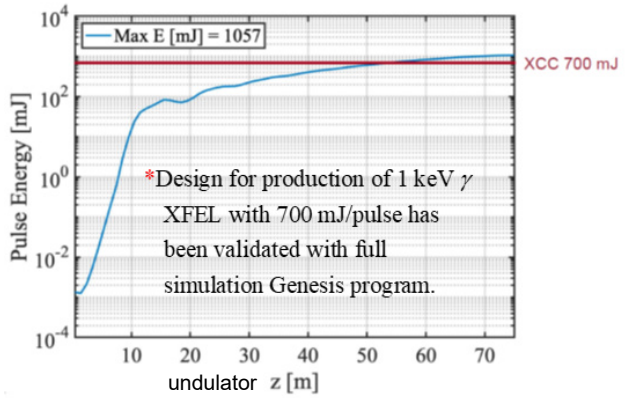

Table of XCC KB mirror parameters

Focal Size (nm)	Photon Energy (eV)	Rayleigh Range (um)	RMS Source Size (um)	AOI (deg)	Max E w/ 10x SF (J)	Substrate Length (m)	Unfocused Beam Size (mm)	Source Distance (m)	Reflectivity	Focal Length (m)	IP Distance from Mirror (m)
50	1000	4.5	10	1.30	0.31	1.00	11.34	487	0.872	1.032	0.532
100	1000	18.2	10	0.90	0.68	1.50	11.78	505	0.926	2.144	1.394
50	2000	9.1	10	0.80	0.54	1.00	6.98	600	0.933	1.27	0.770
100	2000	36.4	10	0.60	1.05	1.40	7.33	629	0.967	2.668	1.968
50	2000	9.1	10	0.65	1.21	1.50	8.51	731	0.962	1.548	0.798
100	2000	36.4	10	0.50	2.14	2.00	8.73	750	0.976	3.176	2.176
40	4000	11.6	10	0.4	1.06	1.13	3.93	675	0.982	1.143	0.581
70	4000	35.7	10	0.3	2.40	1.50	3.93	675	0.992	2.001	1.251
40	4000	11.6	10	0.4	2.39	1.50	5.24	899	0.982	1.525	0.775
70	4000	35.7	10	0.3	4.27	2.00	5.24	899	0.992	2.668	1.668

Mirror Damage Limit (single pulse)

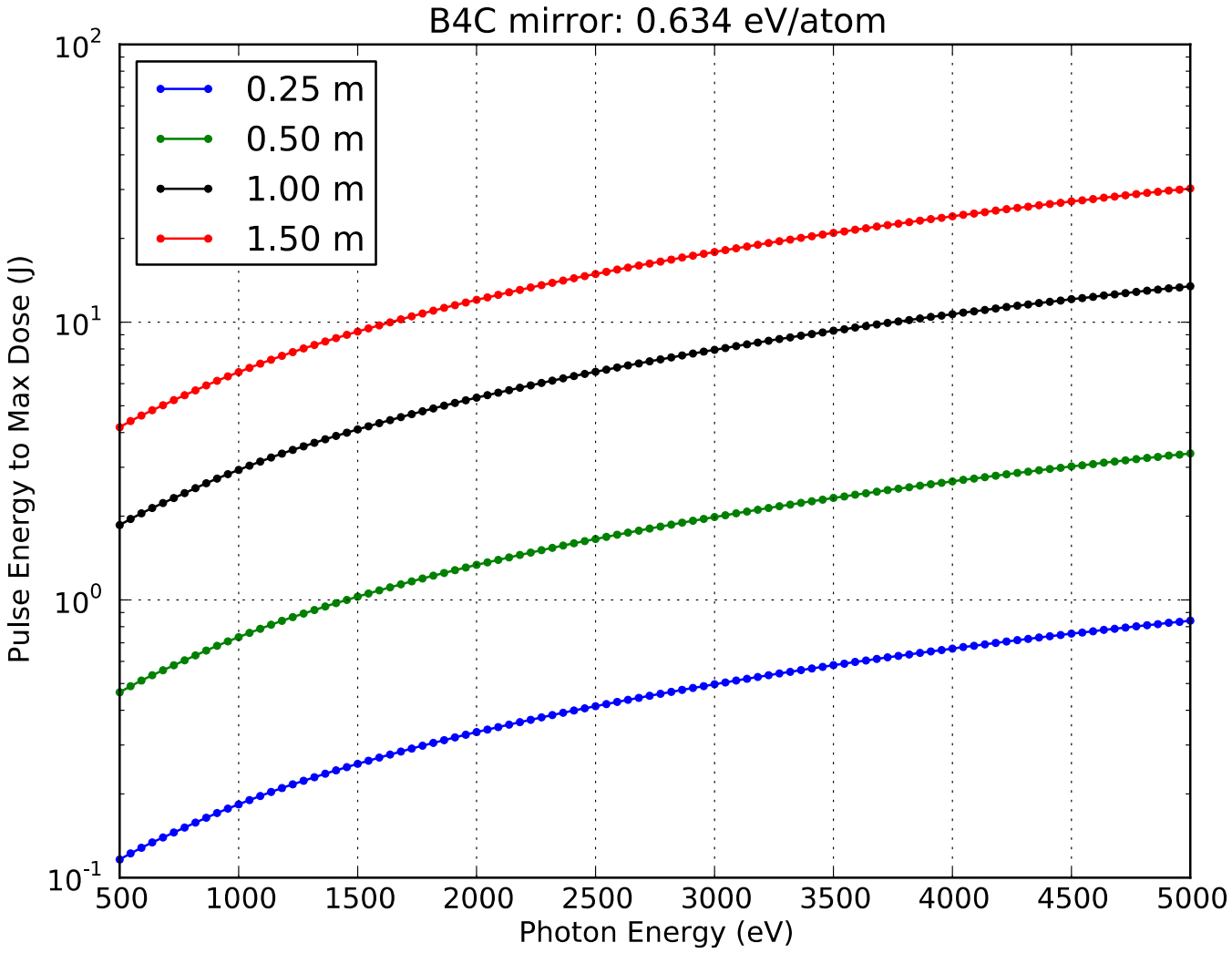

- Boron carbide is the highest damage threshold coating and is used for this calculation
- Assumes the incident fwhm beam size is ½ the substrate length
- No safety factor is included in these calculations – 5-10x below this value should be planned for
- Calculation is weakly dependent on incident angle below the mirror cutoff (0.3 deg AOI used)

A large mirror (> 1 m) is needed to survive ~ 1 J pulse energies

Mirror Reflectivity

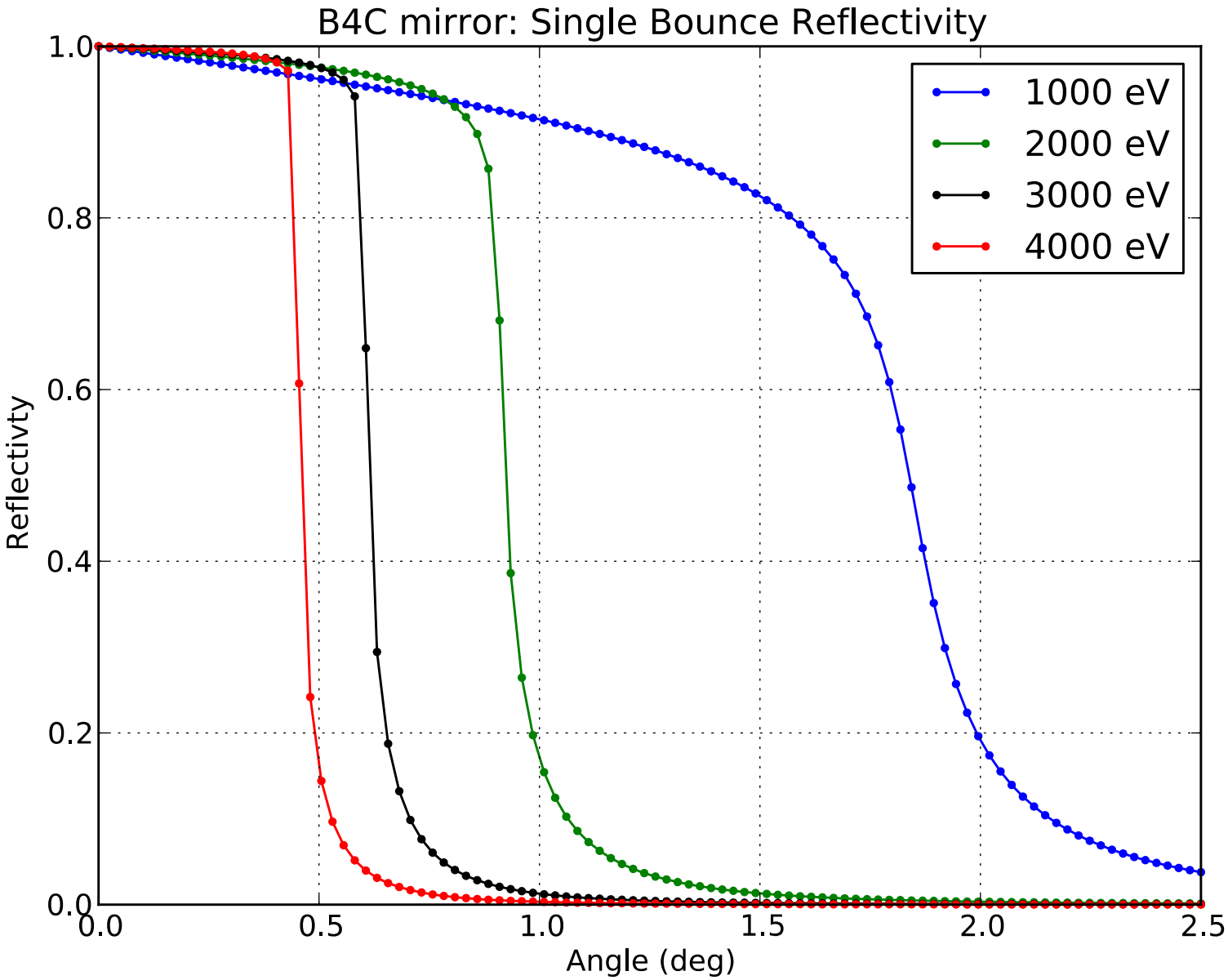

XCC Schematic with 1.4 km line between XFEL and KB mirrors

Demagnify 20 μm FWHM
XFEL beam at undulator exit
to 70 nm FWHM at Compton IP

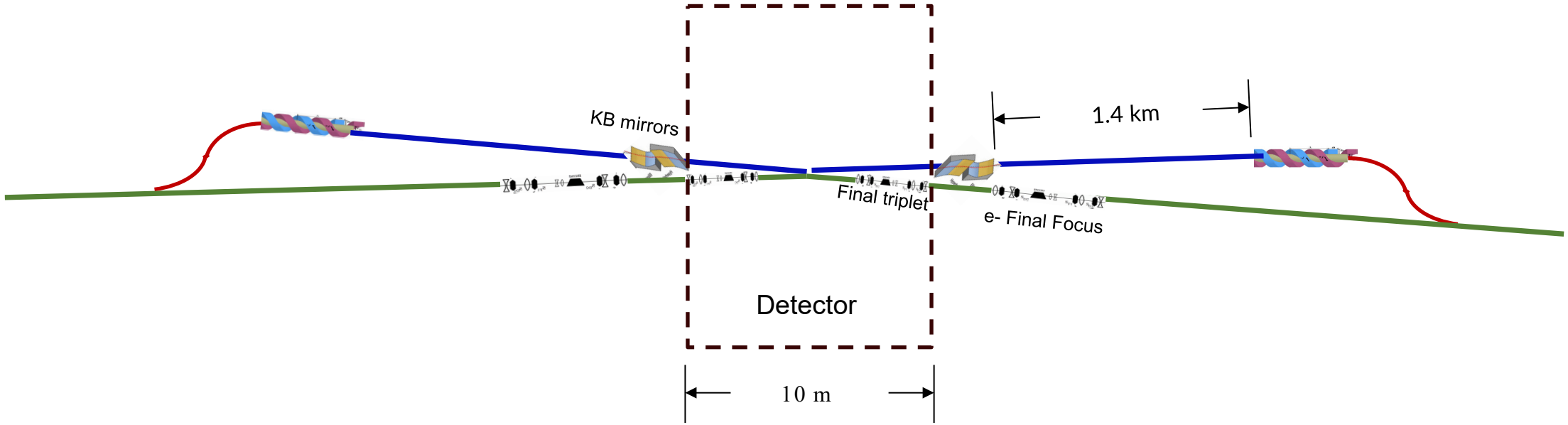

Beam Delivery and Machine Detector Interface at XCC

BDS Accelerator Issues Related to Getting Four Particle Beams In and Out of IP Region

(1) Crossing angle and Aperture of final quad (for 2 mrad crossing angle choice, e^+, e^-, γ from primary & Compton IP's must pass through this aperture; for 20 mrad angle need collimators to protect final quad)

(2) L*, KB mirror length and location

(3) Shared vacuum pipe: point of entry of XFEL beam into e^- beampipe, passing of electron beam through KB mirror chamber (?), beam dump design

Detector issues due to backgrounds from e^+, e^-, γ produced at Compton IP's and primary IP:

(1) Vertex detector inner radius (incoherent e^+e^- pairs from primary IP - same situation as e^+e^- linear colliders)

(2) Beampipe X_0 (moderate soft X-ray flux from Compton IP's $|\cos\theta| < 0.95$)

(3) Forward boundaries of the main tracker/calorimeter and solid angle coverage of forward detector (large hard X-ray flux from Compton IP's $|\cos\theta| > 0.95$)

Event Simulation

Higgs self-couping analysis

of $\gamma\gamma \to HH$ at $\sqrt{s} = 380$ GeV

Cain $(x1, x2)$ spectra is now interfaced to Whizard 3.15 . Data sets such as the following have been produced at $\sqrt{s}$=380 GeV:

$\gamma\gamma \to HH$ $\gamma\gamma \to qq$ $\gamma\gamma \to tt$

$\gamma\gamma \to ZZ$ $\gamma\gamma \to W^+W^-$

$e^-\gamma \to \nu W$ $e^-\gamma \to \nu q\bar{q}W$ $e^-\gamma \to e^-q\bar{q}W$

$e^-\gamma \to e^-Z$ $e^-\gamma \to \nu q\bar{q}Z$ $e^-\gamma \to e^-q\bar{q}Z$

$e^-\gamma \to e^-H$ $e^-\gamma \to \nu q\bar{q}H$ $e^-\gamma \to e^-q\bar{q}H$

In addition the $\gamma\gamma \to$ *hadrons* simulation used with Whizard 1.95 has been interfaced to Whizard 3.15 so pileup is also included.

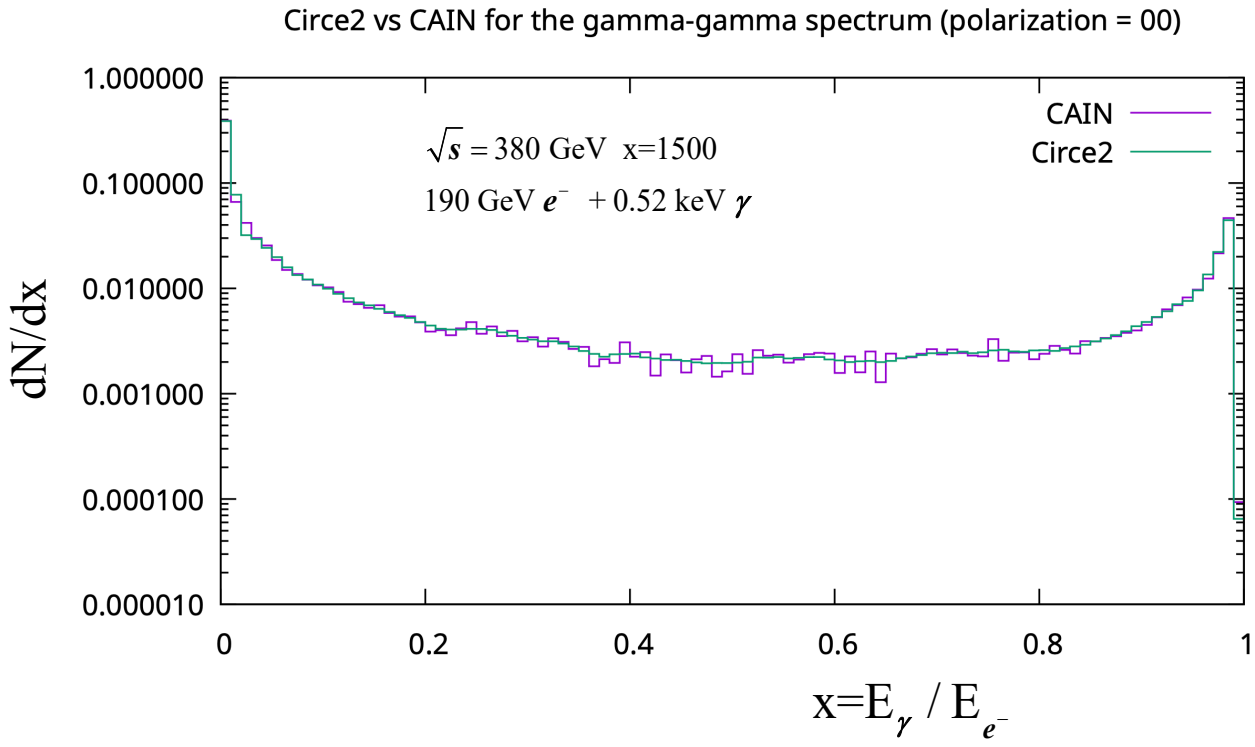

Future Work

- Explore more Compton Configurations (more values of x) and compare $\gamma\gamma$ $e^-\gamma$ e^+e^- spectra with that of e^-e^- Collider.
- Verify with other programs that trident process is responsible for reduction EMfield for very high x and, in general verify, that CAIN luminosity spectra is valid.
- Once converge on Compton Configuration, start producing CAIN + Whizard simulations for beam-beam and machine backgrounds
- Also define scope of accelerator / laser R&D once the Compton Configuration is settled.

Backup Slides

TESLA TDR $\gamma\gamma$ Collider Specifies 34 mrad Crossing Angle

The crossing angle for the TESLA $\gamma\gamma$ collider is discussed in section 1.4.4.2 of

TESLA TDR, Part VI, Chapter 1: The Photon Collider at TESLA

The concern is low energy, large angle particles striking the quads. For fixed $\sqrt{s_{\gamma\gamma}}$ the maximum disruption angle $\vartheta_{\max}$ is given by $\vartheta_{\max} \propto \dfrac{x}{\sqrt{(1+x)\sigma_c(x)}}$ where $\sigma_c(x)$ is the Compton cross section with leading term $\sigma_c(x) \propto \dfrac{1}{x}$.

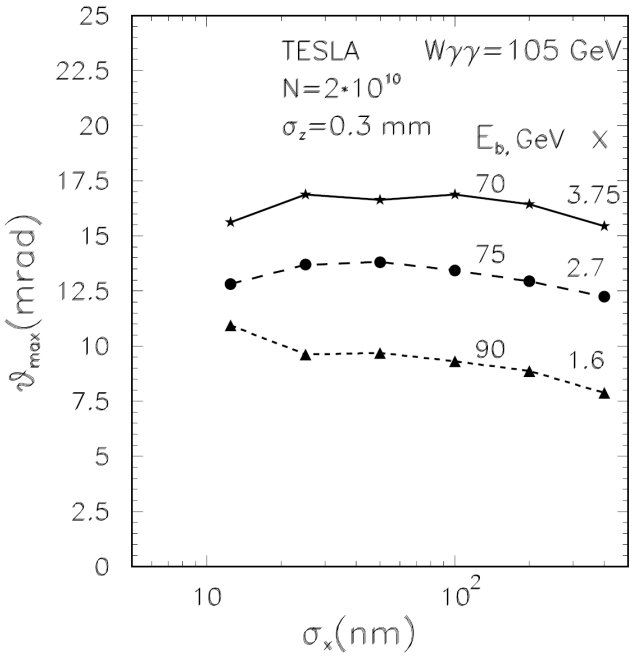

They conclude that for a fixed laser λ=1.06 μm and 200 GeV $\leq \sqrt{s_{\gamma\gamma}} \leq$ 500 GeV, the the maximum disruption angle is $\vartheta_{\max} \approx 14$ mrad, and they set the crossing angle at $\theta_c = 34$ mrad.

Let's check this with CAIN. Calculate energy incident on 6 cm dia. cryostat at L*=3m.

Use parameters for TESLA TDR $\sqrt{s_{\gamma\gamma}} = 500$ GeV, $x = 4.5$

		TESLA-500,$\gamma\gamma$
Repetition rate	f_{rep} [Hz]	5
Beam pulse length	T_P [μs]	950
RF-pulse length	T_{RF} [μs]	1370
No. of bunches per pulse	n_b	2820
Bunch spacing	Δt_b [ns]	337
Charge per bunch	N_e [10^{10}]	2
Emittance at IP	$\gamma\varepsilon_{x,y}$ [10^{-6}m]	3, 0.03
Beta at IP	$\beta^*_{x,y}$ [mm]	4, 0.4
Beam size at IP	$\sigma^*_{x,y}$ [nm]	157, 5
Bunch length at IP	σ_z [mm]	0.3
Geometric luminosity	L_{geom} [10^{34}cm^{-2}s^{-1}]	5.8
Effective $\gamma\gamma$ luminosity	$L_{\gamma\gamma}$ [10^{34}cm^{-2}s^{-1}]	0.6

Table 1.3.2: *Beam parameters for the $\gamma\gamma$ option. The effective luminosity takes into account only the high energy peak of the luminosity spectrum ($E_{cm,\gamma\gamma} \approx 400\,GeV$), see part VI, chapter 1 for details.*

$2E_0$ [GeV]	200	500	800
λ_L [μm]/x	1.06/1.8	1.06/4.5	1.06/7.2
t_L [λ_{scat}]	1.35	1	1
$N/10^{10}$	2	2	2
σ_z [mm]	0.3	0.3	0.3
$f_{rep} \times n_b$ [kHz]	14.1	14.1	14.1
$\gamma\epsilon_{x/y}/10^{-6}$ [m·rad]	2.5/0.03	2.5/0.03	2.5/0.03
$\beta_{x/y}$ [mm] at IP	1.5/0.3	1.5/0.3	1.5/0.3
$\sigma_{x/y}$ [nm]	140/6.8	88/4.3	69/3.4
b [mm]	2.6	2.1	2.7
L_{ee} $(geom)$ [10^{34} cm^{-2}s^{-1}]	4.8	12	19
$L_{\gamma\gamma}(z > 0.8z_{m,\gamma\gamma})$[$10^{34}$ cm^{-2}s^{-1}]	0.43	1.1	1.7
$L_{\gamma e}(z > 0.8z_{m,\gamma e})$[$10^{34}$ cm^{-2}s^{-1}]	0.36	0.94	1.3
$L_{e^+e^-}(z > 0.65)$[10^{34} cm^{-2}s^{-1}]	0.03	0.07	0.095

Table 1.4.1: *Parameters of the $\gamma\gamma$ collider based on TESLA. two options.*

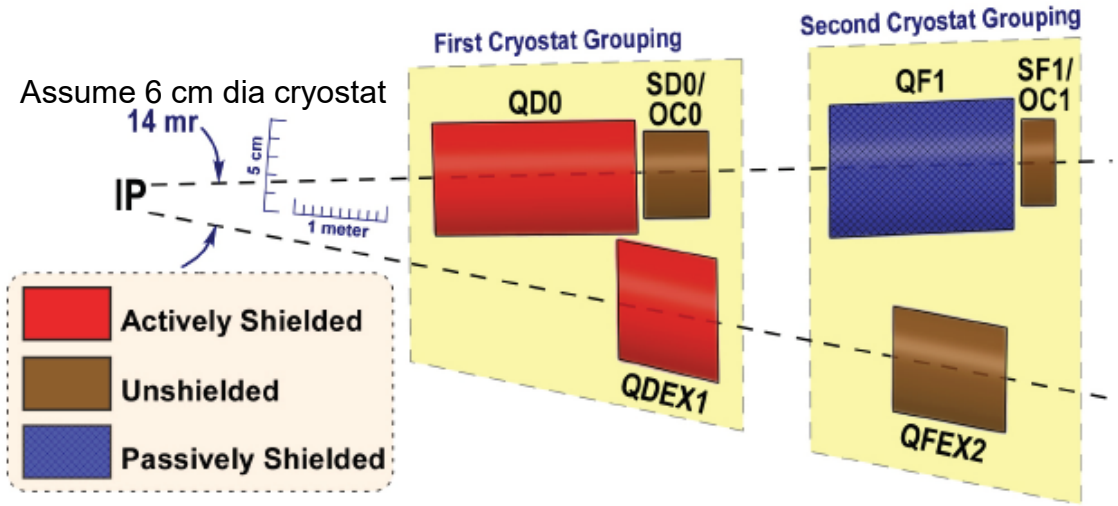

As discussed in Section 1.3.2.1 the 5 μm spot size of the laser beam matches the effective crabbed horizontal beam size of

$\sigma_x = \sigma_z \alpha_c / 2 = 5\ \mu$m for $\sigma_z = 300\ \mu$m and $\alpha_c = 34$ mrad

Hence there is little luminosity degradation for $0 < \alpha_c < 34$ mrad

Not the case for XCC where laser spot size is 21 nm and

$\sigma_x = \sigma_z \alpha_c / 2 = 340\ \mu$m for $\sigma_z = 20\ \mu$m and $\alpha_c = 34$ mrad

TESLA TDR $\gamma\gamma$ Collider $\sqrt{s} = 500$ GeV

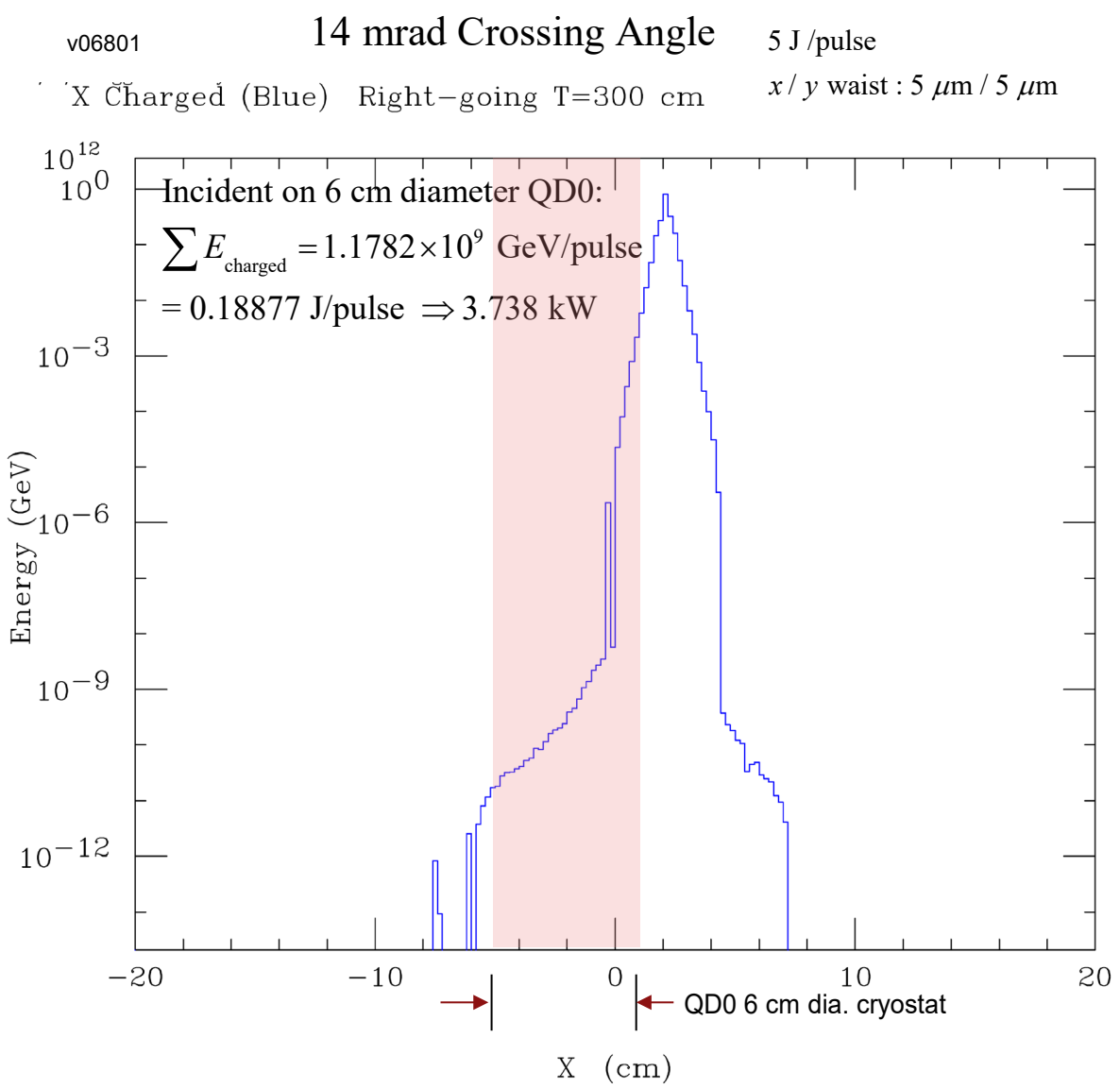

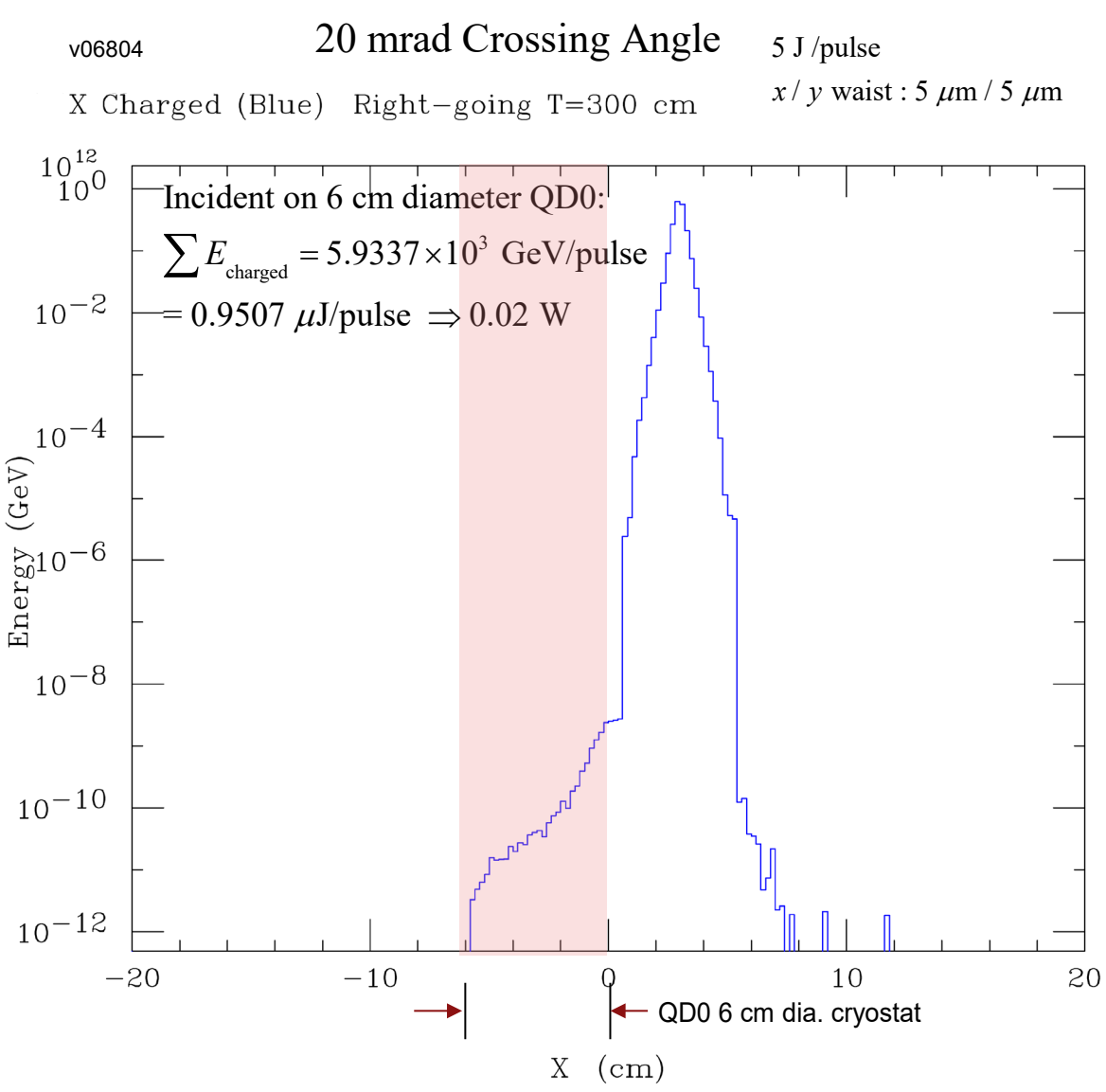

Assuming only few Watts on QD0 is tolerable, we conclude that 14 mrad is insufficient and 20 mrad is the minimum crossing angle.

TESLA TDR $\gamma\gamma$ Collider $\sqrt{s} = 500$ GeV

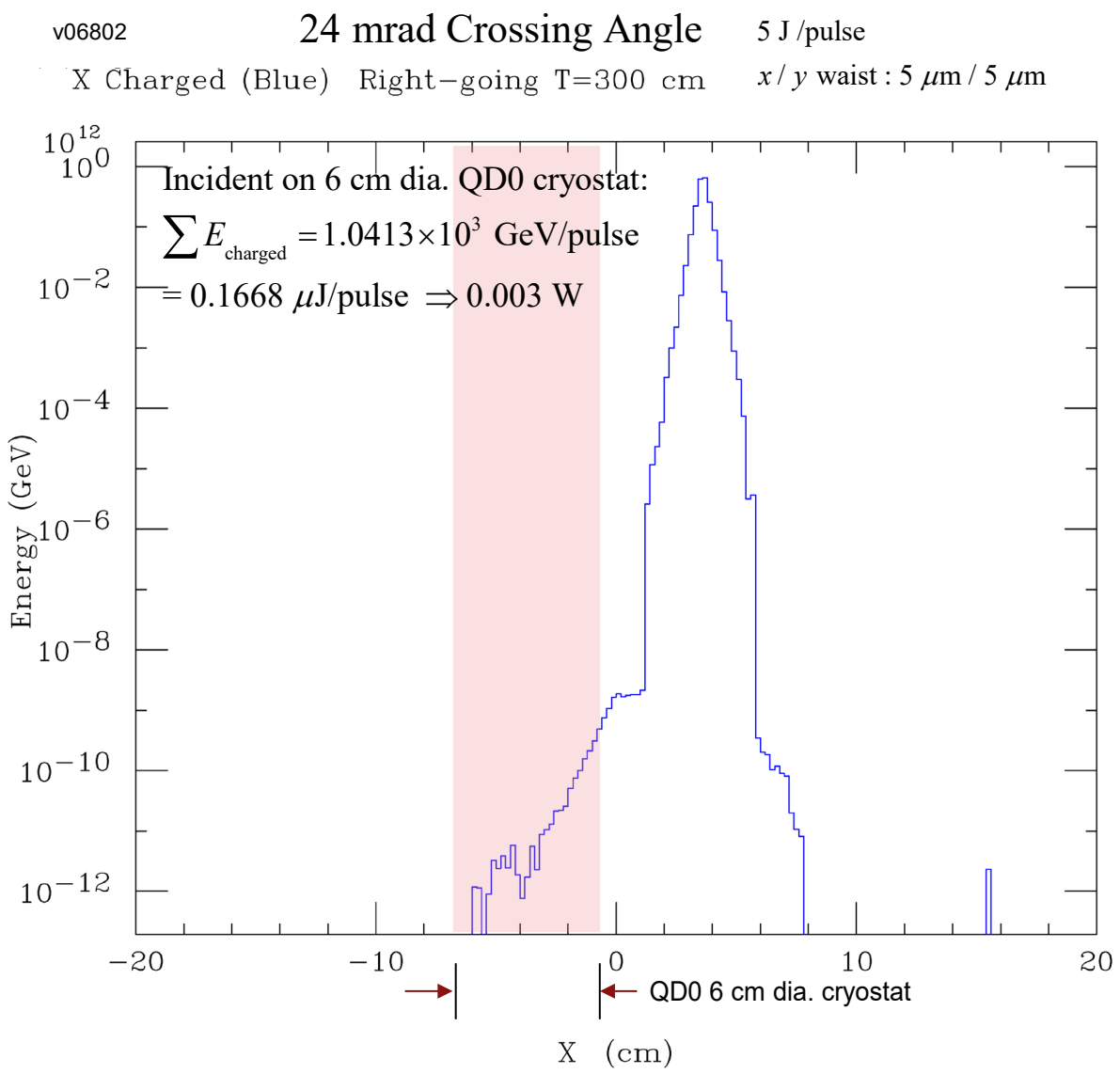

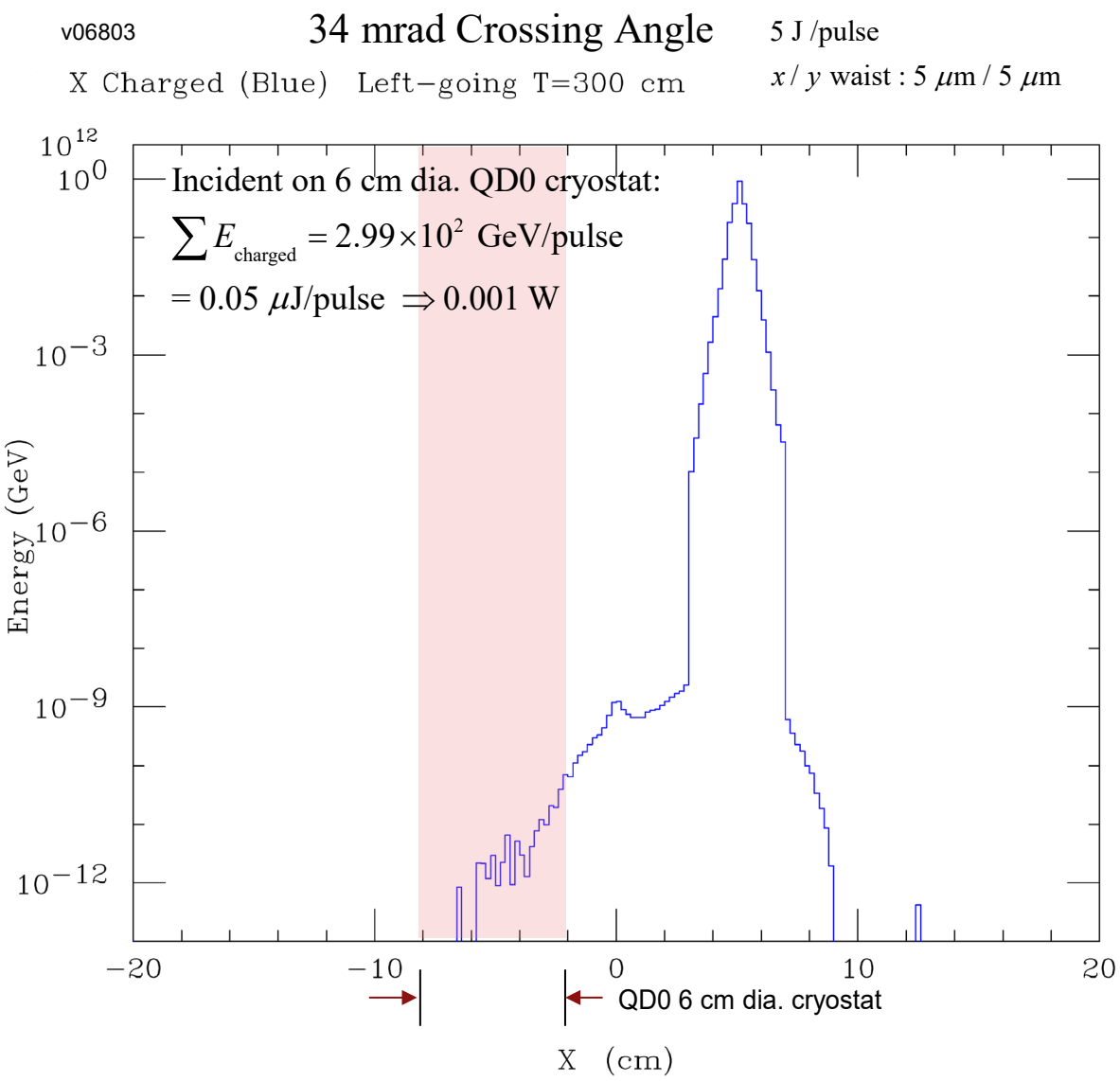

Conclude from CAIN that 24 mrad is more comfortable than 20 mrad and 34 mrad is overkill

XCC $\gamma\gamma$ Collider $\sqrt{s} = 125$ GeV

Increase horizontal laser spot size from 21 nm to 42 (85) nm to better match $\sigma_x = \sigma_z \alpha_c / 2$. Increase pulse energy to maintain laser photon density

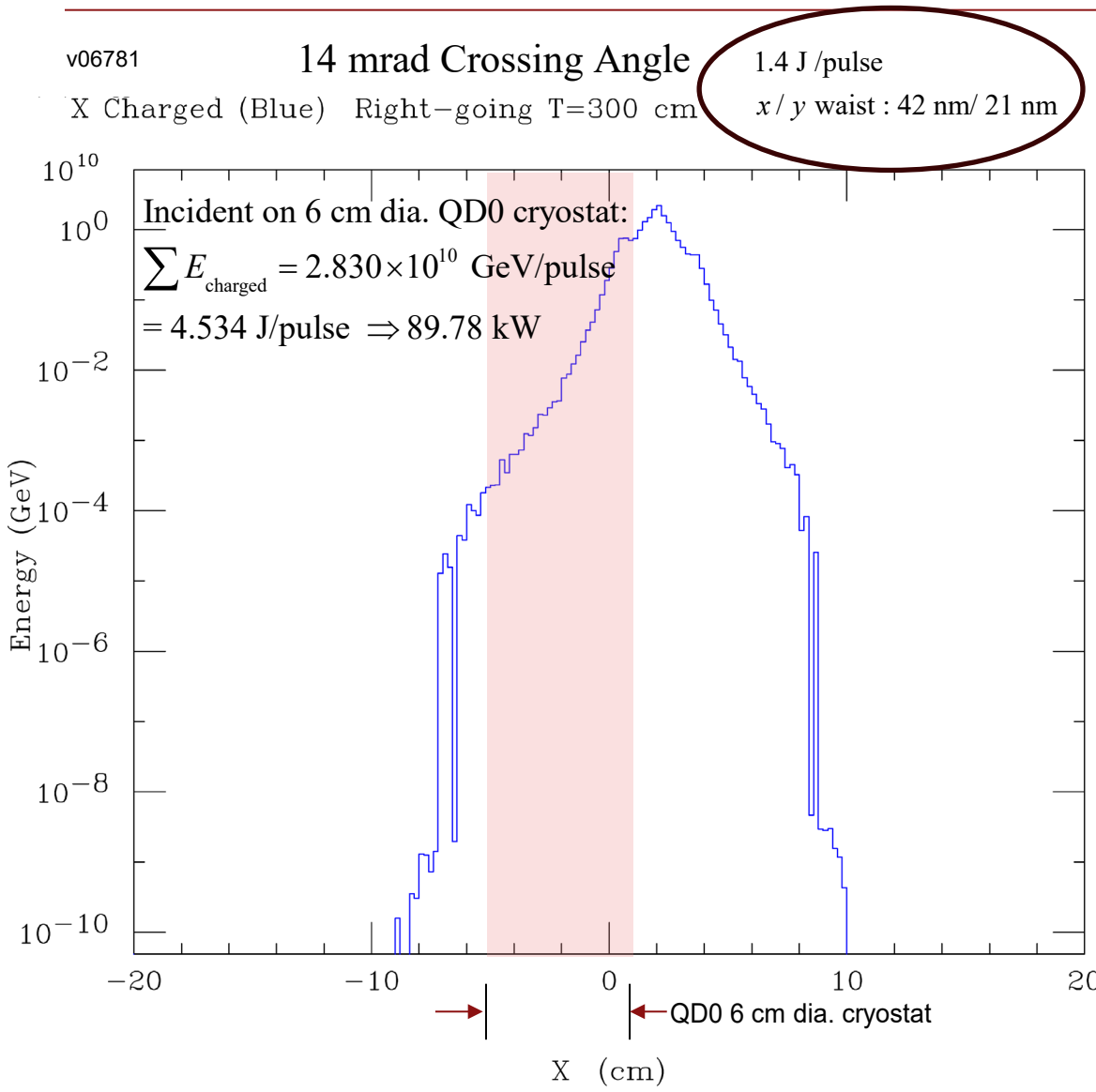

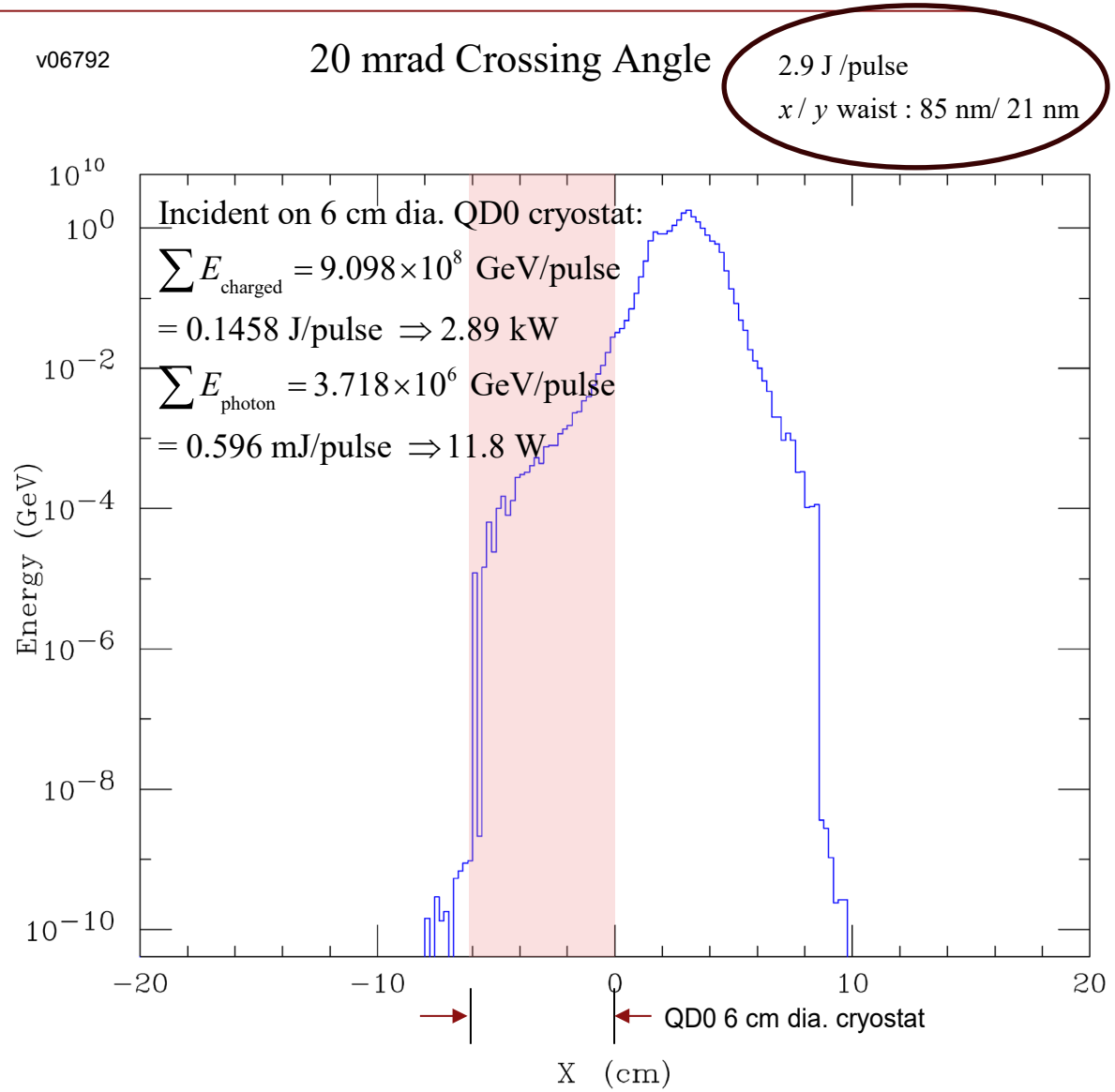

20 mrad will work if collimators are installed to protect QD0; must study size of collimator backscatter into detector

2 mrad crossing angle, L*=1.5 m

CAIN Simulation from IP to Face of Quad at L*=1.5 m, Assume 5 T Solenoid

Incident on Triplet Cryostat:

$\sum E_{\text{charged}} = 4.2306 \times 10^2$ GeV/pulse

$= 0.07\ \mu$J/pulse $\Rightarrow 0.001$ W

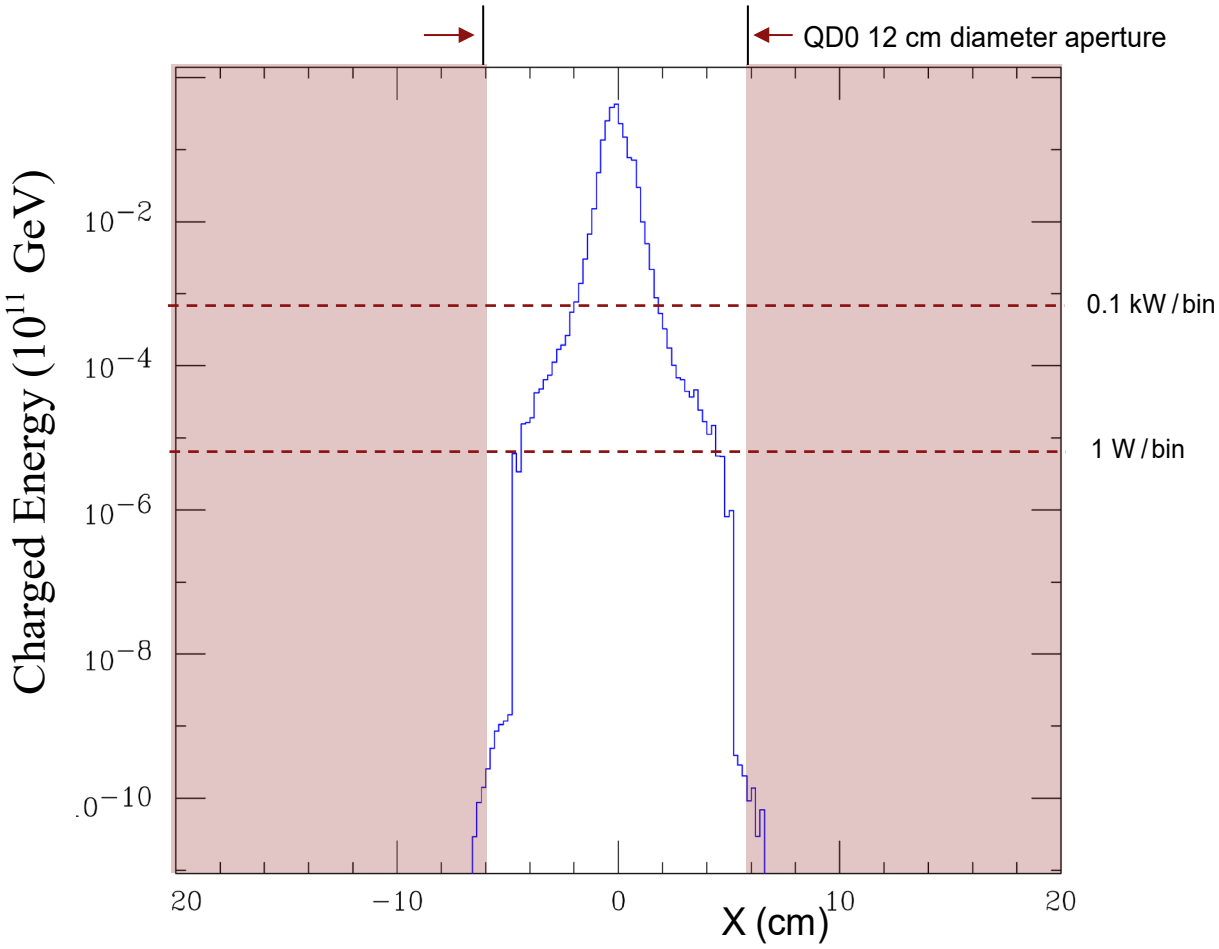

Incident on Triplet Cryostat:

$\sum E_{\text{photon}} = 4.2306 \times 10^2$ GeV/pulse

$= 0.29$ mJ/pulse $\Rightarrow 5.8$ W

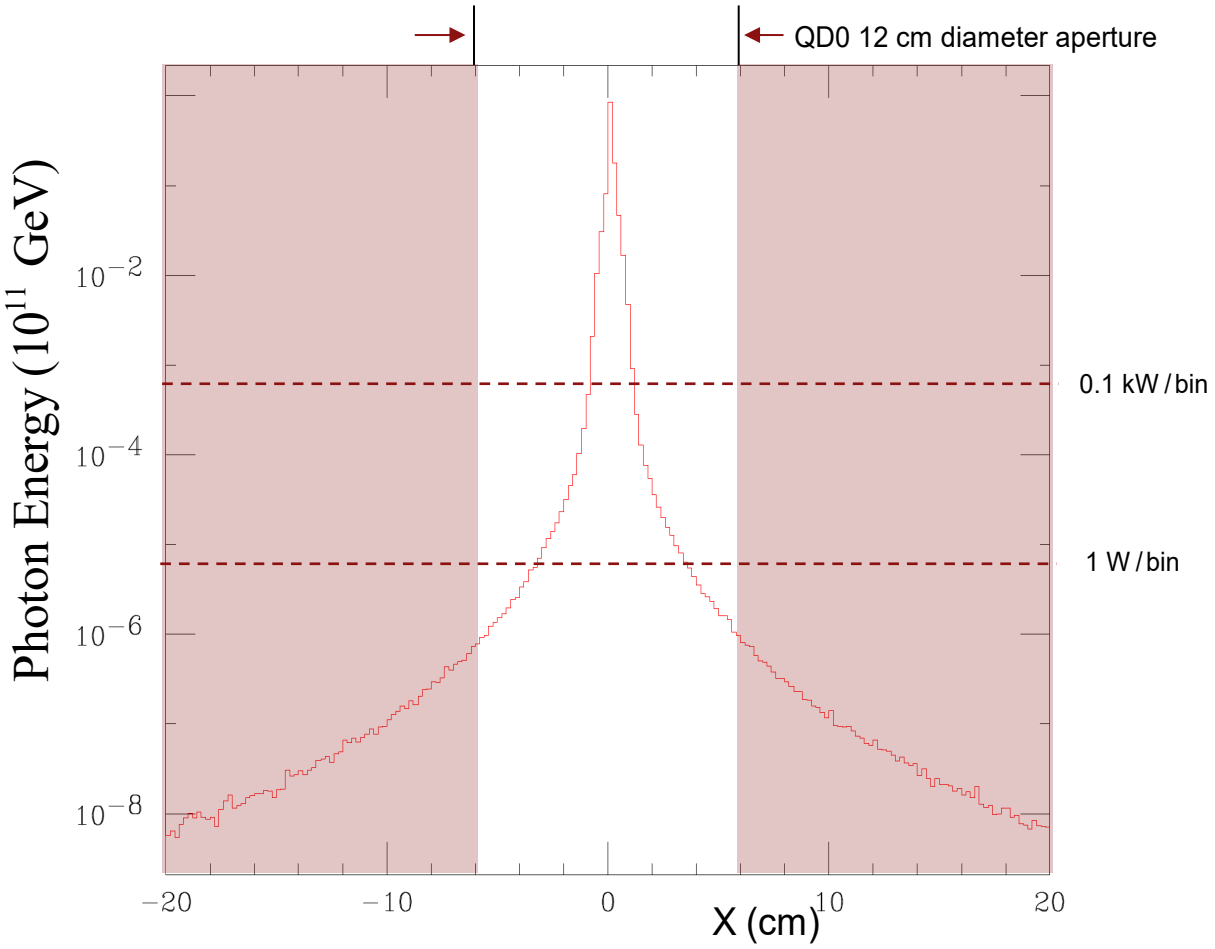

Solution requires large aperture HL-LHC-like final triplet. Significant departure from usual e+e- collider design